Limnol. Oceanogr., 55(6), 2010, 2703–2722

doi:10.4319/lo.2010.55.6.2703

Mercury and methylmercury cycling in sediments of the mid-Atlantic continental shelf and slope

T. A. Hollweg,[a] C. C. Gilmour,[b,*] and R. P. Mason[a]

[a] Department of Marine Sciences, University of Connecticut, Groton, Connecticut
[b] Smithsonian Environmental Research Center, Edgewater, Maryland

Abstract

We present a detailed study of the biogeochemical factors controlling mercury (Hg) distribution, methylmercury (MeHg) production, and MeHg efflux in sediments of the mid-Atlantic continental shelf and slope. The mildly reduced surface sediments of the shelf and slope provide ideal conditions for MeHg production. They are sufficiently reduced to support microbial sulfate reduction, but contain very low dissolved sulfide concentrations. The redox zonation of sediments determined the depth distribution of MeHg production, whereas the bioavailability of inorganic Hg for methylation appeared to be the dominant driver of spatial patterns across the shelf and slope. Sediment total Hg concentrations were well predicted by sediment organic matter (SOM) content, with the highest concentrations of Hg and MeHg in the fine-grained organic clays of the slope. However, SOM-normalized Hg concentrations decreased with distance from shore. The changing character of organic matter with distance from shore appeared to affect Hg partitioning and bioavailability for methylation. The percentage of Hg in sediments as MeHg was well predicted by measured methylation rates, but not by demethylation rates. On the basis of measured concentrations in bottom waters and surficial pore waters, the average diffusive efflux of Hg(II) and MeHg from sediments to coastal waters was estimated to be 26 and 0.8 pmol m^{-2} d^{-1}, respectively. Extrapolated globally, the diffusive input of MeHg from shelf and slope sediments is estimated to be 0.01 Mmol per year. As the actual fluxes can be substantially higher than diffusive fluxes, we suggest that shelf and upper slope sediments are a major source of MeHg to the coastal ocean.

With the marine fisheries contributing more than two thirds to the global fish catch (FAO 2008), it is not surprising that marine and estuarine seafood are the main risk drivers for methylmercury (MeHg) exposure to people (Sunderland 2007; FAO 2008). However, the sources and sinks of Hg and especially MeHg in the oceans and coastal zones remain poorly understood. To better assess risk and better understand how MeHg levels in marine systems might respond to changing Hg loads to the oceans, we studied one of the largest potential sources of MeHg to the coastal zone, de novo MeHg production in continental shelf and slope sediments. Our study system was the mid-Atlantic continental shelf, from about 36° to 38°N, off of Delaware, Maryland, and North Carolina.

Coastal zones and marine surface waters are heavily affected by anthropogenic Hg loads. Sunderland and Mason (2007) estimate that worldwide, surface oceans have been anthropogenically enriched globally by about 25%, and by more than 60% in parts of the Atlantic. An examination of Hg concentrations in the northern Pacific through time suggests that Hg concentrations will double in the surface ocean by the year 2050 at current deposition rates (Sunderland et al. 2009). Thus there is an expectation that MeHg levels in marine fish are elevated in response to increased marine Hg loading, and could decline in time if anthropogenic sources are controlled. MeHg is the Hg species of main concern because of its bioamplification and toxicity (Mergler et al. 2007).

Methylmercury concentrations in aquatic systems are controlled by the balance of methylation and demethylation rates, the bioavailability of Hg and MeHg for transformation, and exchanges between compartments (Munthe et al. 2007). The relative importance of external and internal sources of MeHg has not been quantified for either coastal or open ocean systems. In the coastal zone, major external MeHg sources may include riverine and coastal inputs, atmospheric input (Mason and Benoit 2003), and groundwater inputs (Black et al. 2009). Potential sites of in situ net MeHg production in the coastal zone include production in both the water column and in sediments. Budgets for the Chesapeake (Mason et al. 1999) and one of its subestuaries (Benoit et al. 1998) and for Long Island Sound (Hammerschmidt et al. 2004) suggest that MeHg flux from bottom sediments in these systems exceeds external inputs.

The amount of net MeHg production in the water column remains difficult to assess, although there is increasing evidence for low rates of MeHg production in marine waters at depths of high heterotrophic organic matter remineralization (Monperrus et al. 2007*a*; Cossa et al. 2009; Sunderland et al. 2009), or lower oxygen concentrations (Kirk et al. 2008). Anoxic coastal bottom waters in eutrophic waters (“dead zones”) are another likely source of water-column MeHg production in some coastal zones (C. Gilmour, A. Heyes, and J. Schijf unpubl.)

There is growing evidence of the importance of sediments as sources of MeHg to coastal systems. Although the paradigm of sulfide inhibition of methylation led to the expectation of low net MeHg production in often sulfidic saline sediments, methylation rate constants similar to those observed in freshwater sediments have been measured in estuarine sediments in Chesapeake Bay (Benoit et al.

* Corresponding author: gilmourc@si.edu

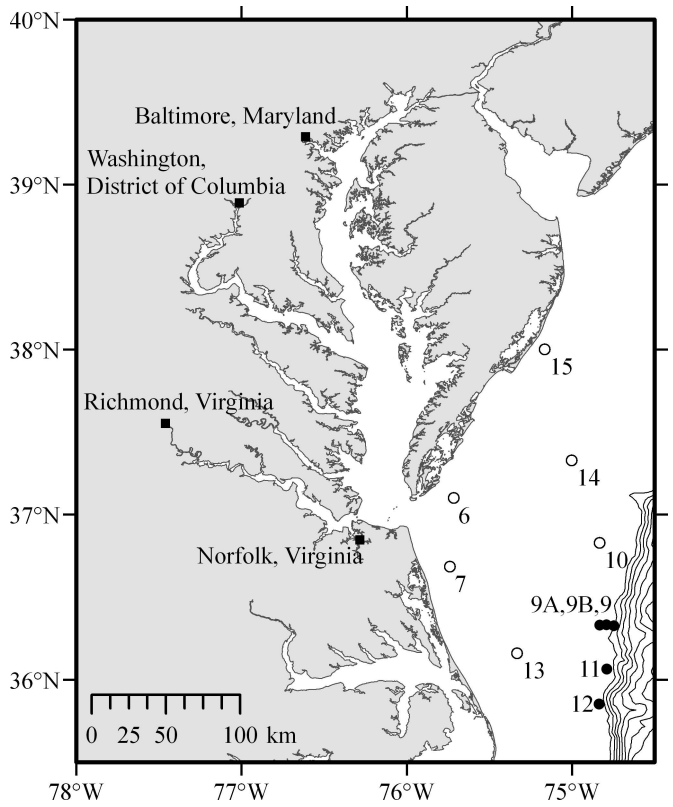

Fig. 1. Location of stations sampled in the mid-Atlantic continental shelf (open circles) and slope (filled circles) during April 2006. Bathymetry contours are every 500 m.

1998; Heyes et al. 2006; Hollweg et al. 2009), in Long Island Sound and New York Harbor (Hammerschmidt and Fitzgerald 2004; Hammerschmidt et al. 2008), in the Bay of Fundy (Sunderland et al. 2006), and the Mediterranean Sea (Monperrus et al. 2007*b*); and in open marine sediments of the southern New England shelf (Hammerschmidt and Fitzgerald 2006), the Mediterranean Sea (Ogrinc et al. 2007), and the mid-Atlantic continental margin (Hollweg et al. 2009). The fraction of total Hg as MeHg in estuarine and marine surface sediments seems to generally average between 0.5% and 2%.

Although MeHg concentrations and production rate constants are negatively correlated with pore-water sulfide in estuarine sediments (Benoit et al. 1999; Hammerschmidt et al. 2008; Hollweg et al. 2009), many saline sediments have a surface layer that is anoxic, but with little or no (low micromolar) dissolved sulfide, above the deeper, more sulfidic zones. These zones often support high levels of microbial sulfate or iron-reducing activity. Physical mixing (Sunderland et al. 2004) and bioturbation of bottom sediments (Benoit et al. 2009), as well as plants in tidal marshes (Mitchell and Gilmour 2008), can also generate anoxic, low-sulfide zones where MeHg production is favored in saline sediments and soils.

Here we explore in detail MeHg distribution, production, and biogeochemistry in sediments of the mid-Atlantic continental margin. This study expands our previous work on mid-Atlantic shelf and slope sediments to include a larger spatial scale and a broader range of sediment characteristics. We also estimate the diffusive flux of MeHg from sediments to the coastal ocean, and assess the importance of these sediments in the global ocean MeHg budget.

Methods

Field sampling—From 07 to 16 July 2006, 11 sites on the mid-Atlantic continental margin were visited on board the RV *Cape Hatteras*. Detailed biogeochemical analyses were performed in the water column and surface sediment (upper 4 cm), primarily focusing on the effects of Fe, S, and C cycling on net MeHg production. These sites covered a broad range of water depths and sediment bottom types (Fig. 1, Table 1). Three of these sites were sampled during four previous cruises (April 2006 and May, July, and September 2005; Hollweg et al. 2009).

Bottom water was sampled ~ 1 m above the sediment surface at Sta. 6, 7, 9, 10, 12, and 14, following clean techniques outlined in Gill and Fitzgerald (1985). Water was collected using acid-washed and deionized (DI) rinsed General Oceanics Go-Flo sampling bottles with Teflon-coated messengers deployed from a Kevlar line. Go-Flo sampling bottles were bagged on deck, taken into a self-contained high-efficiency particulate air-filtered clean van and emptied into acid-cleaned Teflon bottles until processing. Water was filtered through a combusted 0.7-μm glass fiber filter into acid-cleaned Teflon bottles using a dome vacuum filtration setup with acid-cleaned Teflon filter towers. For total mercury (HgT) and MeHg analyses, aliquots of water were collected in separate Teflon bottles, acidified to ~ 0.5% with trace-metal-grade HCl, and stored in the dark. For dissolved organic carbon (DOC) analysis, aliquots of water were collected in small Teflon vials and frozen.

Sediments were sampled using an Ocean Instruments Mk III 50 × 50 cm box corer, which was modified to increase core recovery, as described in Hollweg et al. (2009). Box cores with substantially turbid overlying water were rejected. Box-cored sediments were subsampled with 4.8-cm polycarbonate tubes, and stored at either ambient bottom-water temperature (for methylation and demethylation incubation experiments) or on ice (bulk-phase and pore-water collection).

For bulk-phase and pore-water collection, intact sediment cores were placed in an oxygen-free Coy glove box for processing within 2 h after the box cores were subsampled (Hollweg et al. 2009). Bulk-phase analyses including Fe(II), Fe(III), acid-volatile sulfur (AVS), and chromium-reducible sulfur (CRS). For pore-water collection, sediment was placed in acid-cleaned and DI-rinsed Nalgene polystyrene filter units (0.2-μm cellulose nitrate filter and a combusted 0.7-μm glass fiber prefilter), and pore water was extracted via vacuum filtration. Pore-water analyses included HgT and MeHg (acidified to ~ 0.5% with trace-metal-grade HCl), sulfide (preserved in sulfide antioxidant buffer), Fe and Mn (acidified to ~ 0.2% with trace-metal-grade HCl), anions (frozen), nutrients (frozen), and DOC (frozen).

Mercury methylation and MeHg demethylation incubations—Mercury methylation and MeHg demethylation

Table 1. Station location, depth, and bottom water properties for each sampling date.

Month	Year	Site	Depth (m)	Temperature (°C)	Salinity	Dissolved oxygen (mg L^{-1})	Latitude (°N)	Longitude (°W)
May	2005	6	16	7.7	31.9	8.1	37.0822	−75.7180
Jul	2005	6	16	16.8	30.9	7.4	37.0936	−75.7054
Sep	2005	6	14	15.5	31.3	4.8	37.0936	−75.7053
Apr	2006	6	16	12.1	32.1	8.3	37.0945	−75.7040
Jul	2006	6	16	17.0	32.1	6.9	37.1020	−75.7150
Jul	2005	7	15	14.4	31.4	7.7	36.6912	−75.7404
Sep	2005	7	14	17.7	31.4	5.2	36.6973	−75.7303
Apr	2006	7	15	13.4	31.9	8.5	36.6912	−75.7413
Jul	2006	7	17	14.0	33.1	8.1	36.6883	−75.7388
Jul	2005	9*	722	12.8	35.2	6.5	36.3312	−74.7384
Sep	2005	9*	650	5.3	35.0	4.5	36.3355	−74.7454
Apr	2006	9*	819	4.4	35.0	8.2	36.3350	−74.7344
Jul	2006	9*	646	5.0	35.0	7.2	36.3265	−74.7447
Jul	2006	9A*	85	15.0	35.3	6.5	36.3308	−74.8303
Jul	2006	9B*	107	14.0	35.4	5.4	36.3320	−74.7888
Jul	2006	10	48	14.0	34.7	6.2	36.8318	−74.8330
Jul	2006	11*	227	12.0	35.3	4.3	36.0628	−74.7877
Jul	2006	12*	600	5.0	35.0	6.6	35.8520	−74.8335
Jul	2006	13	32	15.5	34.2	7.8	36.1633	−75.3315
Jul	2006	14	38	14.0	34.1	7.6	37.3320	−75.0012
Jul	2006	15	19	14.0	31.2	7.3	38.0035	−75.1650

* Slope stations.

rates were estimated by introducing enriched stable Hg isotopes ($Me^{199}Hg$ and ^{201}Hg) into intact sediment cores (Hintelmann and Evans 1997; Mitchell and Gilmour 2008). Enriched stable mercury isotopes were obtained from Oak Ridge National Laboratory, with a purity of 91.95% for ^{199}Hg and 98.11% for ^{201}Hg. $Me^{199}Hg$ was synthesized using methylcobalamin (Hintelmann and Ogrinc 2003).

In the field, stock solutions of ^{201}Hg and $Me^{199}Hg$ were diluted with 0.22-μm-filtered bottom water and equilibrated for an hour at ambient bottom-water temperature before use. After the equilibration time, the isotope supplements were injected into the sediment cores at 1-cm horizontal increments (Gilmour and Riedel 1995). For the July 2005 cruise, injections were made to 5 cm down core and 1 cm above the sediment surface in the overlying water. Methylation and demethylation rate experiments were performed separately, in triplicate, with a 4-h incubation time. After incubation, the sediment cores were sectioned and immediately frozen on dry ice. For methylation rate experiments, the ^{201}Hg supplement ($\sim$ 280 pmol Hg cm^{-3} sediment) increased the total Hg content 1.5× in organic-rich sediment (> 1% loss on ignition; LOI) and 8.4× in sandy sediment (< 1% LOI). For demethylation rate incubation experiments, the $Me^{199}Hg$ supplement ($\sim$ 56 pmol MeHg cm^{-3} sediment) increased the MeHg content 32× in organic-rich sediment and 97× in sandy sediment. For the first four cruises, methylation and demethylation rate experiments were performed together, in duplicate, with a 2-h incubation time, as discussed in Hollweg et al. (2009).

The methylation rate constant (k_{meth}) was determined by measuring the formation of excess $Me^{201}Hg$ from the ^{201}Hg supplement, whereas the demethylation rate constant (k_{demeth}) was determined by measuring the loss of excess $Me^{199}Hg$, as discussed in Hintelmann et al. (2000), Martin-Doimeadios et al. (2004), and Heyes et al. (2006). For the calculation of the rate constants, it was assumed that methylation and demethylation rates were both pseudo-first-order kinetic reactions (Hintelmann et al. 2000). Our equations for methylation and demethylation rate calculations are given in Hollweg et al. (2009).

In this study, the detection limit (DL) for k_{meth} was estimated to be 0.001 d^{-1} for organic-rich sediments (> 1% LOI) and 0.0002 d^{-1} for sandy sediments (< 1% LOI), using similar calculations to those described in Mitchell and Gilmour (2008). Similarly, the DL for k_{demeth} was estimated to be 0.13 d^{-1} for both organic-rich and sandy sediments. For laboratory analysis of ambient Hg standards, the average relative standard deviation of the ratios of 201 : 202-Hg and 199 : 202-Hg were 2.3% and 2.5%, respectively (n = 12). At all stations, our measured rate constants for k_{meth} and k_{demeth} were above these estimated DLs.

Mercury and MeHg analysis—Total Hg analysis was conducted following digestion, $SnCl_2$ reduction, and gold-trapping techniques (Gill and Fitzgerald 1987; EPA 2002). For the analysis of HgT in the pore water and water column, Hg water samples were reduced and trapped manually using bubblers. Gold-coated traps were heated and Hg^0 was introduced directly into either a Perkin Elmer dynamic reaction cell (DRC) II inductively coupled plasma mass spectrometer (ICP-MS) for pore-water analysis (Smithsonian Environmental Research Center, SERC) or a Tekran cold vapor atomic fluorescence (CVAFS) mercury detector 2500 for water column analysis (University of Connecticut). Concentrations of ambient HgT were calculated using external standards. The running average DL for HgT in 10- to 30-mL pore-water samples was

0.66 pmol L^{-1} on the basis of 3× the standard error of filter blanks. Recovery of supplements (50 pg per 20 mL) averaged 112%. The average relative standard deviation (RSD) of laboratory replicates was 11%.

For sediment HgT analysis, samples were digested in hot acid (3 : 7 mixture of H_2SO_4 : HNO_3) followed by BrCl, as discussed in more detail in Hollweg et al. (2009). Digested samples were analyzed at SERC and the University of Connecticut on a Perkin Elmer ELAN DRCII ICP-MS with an attached flow injection auto sampler system. An enriched isotope internal standard (^{200}HgCl) was added the night before the digestion (Hintelmann and Ogrinc 2003). The concentration of ambient Hg and the excess abundance of each isotope were calculated using isotope dilution. For this cruise, the RSD of laboratory duplicates was 2.8% (n = 19), whereas the RSD of field triplicate cores was 15%. Recovery of a certified reference matieral (CRM), estuarine sediment MESS-3 from the Canada National Research Council (455 ± 45 pmol g^{-1}), was 453 ± 8 pmol g^{-1} (99.6% recovery; n = 13). The DL for HgT analysis in 50 mL of digested sample was 0.17 pmol g^{-1} (n = 15) on the basis of 3× the standard error of laboratory blanks.

MeHg analysis followed distillation, ethylation, and gas-chromatographic separation techniques (Method 1630, EPA 2001), as discussed in Hollweg et al. (2009) and Mitchell and Gilmour (2008). Sediment and pore-water analyses were performed on a Perkin Elmer DRCII ICP-MS at the University of Connecticut and SERC, respectively, using isotope dilution (Hintlemann and Evans 1997; Hintelmann and Ogrinc 2003; Mitchell and Gilmour 2008). Water-column sample analyses were performed on a Tekran CVAFS mercury detector 2500 at the University of Connecticut using external standards. For sediment MeHg, the RSD for laboratory duplicates was 10% (n = 13), the RSD for field triplicates was 18.6%, and supplement recoveries averaged 100.6% ± 10.3% (n = 8). Recovery of a CRM (estuarine sediment, International Atomic Energy Agency; IAEA-405; 27.45 ± .53 pmol g^{-1}) was 24.6 ± 6.2 pmol g^{-1} (90% recovery, n = 23). The DL for MeHg in sediments (in 20 mL of distillate) was 0.017 pmol g^{-1} (n = 7) on the basis of 3× the standard error of laboratory blanks. For water samples, MeHg supplement recoveries averaged 88.2% (n = 17) and the DL (in 120 mL of distillate) was 0.19 pmol L^{-1} (n = 29) on the basis of 3× the standard error of laboratory blanks. For the data reported in this manuscript, the running average DL for MeHg in 30- to 40-mL pore-water samples was 0.26 pmol L^{-1} on the basis of 3× the standard error of filter blanks.

Ancillary analyses—Additional analyses included AVS-CRS and 0.5 mol L^{-1} HCl-extractable FeII and FeIII in sediments; and filterable DOC, sulfide, sulfate, chloride, phosphate, nitrate, iron, and manganese in pore waters. Detailed methods for additional analyses are given in Mitchell and Gilmour (2008) and Hollweg et al. (2009).

Dissolved inorganic Hg and MeHg speciation: Thermodynamic modeling—To assess biogeochemical controls on net MeHg production and calculate the diffusive flux of Hg and MeHg from shelf sediments, the aqueous speciation of both complexes in sediment pore water and overlying water was modeled using MINEQL+ chemical speciation software version 4.5 (Schecher and McAvoy 2001). For these models, we assumed equilibrium with the solid phase, and therefore did not include solid-phase interactions. We decided on complexes and formation constants on the basis of the large body of literature demonstrating that sulfides and organic thiols are the main drivers of aqueous Hg and MeHg complexation (Dyrssen and Wedborg 1991; Benoit et al. 1999; Benoit et al. 2001*b*). Formation constants are listed in Table 2. The validity of the stability constants used in this paper is supported by a more detailed speciation modeling study (Hollweg 2010), which includes comparisons of different speciation models to field data in the sediments of our study area. This analysis supports the use of the higher stability constant for HOHgSH in the speciation model presented in this paper, as used by others (Benoit et al. 1999, 2001*a*). However, we do acknowledge that there are controversies over the stability constants for HOHgSH and Hg bound to organic matter. For example, Skyllberg (2008) proposed that the stability constant for HOHgSH has been dramatically overestimated, and suggested using a lower stability constant for future speciation modeling. In addition, as discussed in Skyllberg (2008), the choice of a stability constant (K) for Hg bound to organic matter (Hg-OM) remains uncertain. For this paper, we modeled the Hg-OM interaction as Hg bound to two reduced thiol groups, $Hg(SR)_2$, with a log K of 42 as suggested by Skyllberg (2008). This stability constant is similar to what has been previously suggested by others (Dyrssen and Wedborg 1986; Benoit et al. 1999). For example, a log K of 41.6 was determined in a titration experiment of thiols by Dyrssen and Wedborg (1986) and using a log K of either 42 or 42.5 was the best fit of the speciation model to field data for the Patuxent River and the Florida Everglades, respectively, by Benoit et al. (1999). However, we note that the interaction of Hg-S complexes with organic matter is not entirely understood, as recent experimental work has shown an interaction between OM and Hg(II) in the presence of dissolved sulfide (Hsu-Kim and Sedlak 2005; Miller et al. 2007; Deonarine and Hsu-Kim 2009), which thermodynamic models would not accurately predict.

Measured concentrations of total filterable sulfide, Hg(II), and MeHg and pH, and an estimated concentration of reduced thiol groups (RSH) were included in the thermodynamic speciation model. The concentration of RSH in dissolved organic matter (DOM) was estimated from the DOC concentration and the RSH : DOC ratio, as discussed below. The DOC concentration was measured in the bottom water and estimated in the sediment using a linear relationship between bulk-phase organic carbon (POC) and DOC concentration (DOC = POC × 0.132 + 482; r^2 = 0.74; DOC in units of μmol L^{-1} and POC in units of μmol g^{-1}) on the basis of data in Burdige and Homstead (1994) and Alperin et al. (1999). DOC and Hg concentrations in the bottom water and pore water are shown in Tables 3 and 4, respectively. The concentration of RSH was estimated by assuming the ratio of RSH to DOC was 0.25 mass %. This value was based on the average

Table 2. Thermodynamic stability constants (K) for MeHg and Hg(II) complexes used in equilibrium modeling.

Equilibrium reaction	Log K	References
$MeHg^+ + RS^- = MeHgSR$	16.5	Karlsson and Skyllberg (2003)
$MeHg^+ + HS^- = MeHgSH$	14.5	Dyrssen and Wedborg (1991)
$MeHgSH = MeHgS^- + H^+$	−7.5	Dyrssen and Wedborg (1991)
$MeHg^+ + OH^- = MeHgOH$	9.37	Schwarzenbach and Schellenberg (1965)
$MeHg^+ + Cl^- = MeHgCl$	5.25	Schwarzenbach and Schellenberg (1965)
$Hg^{2+} + OH^- = HgOH^+$	10.67	Dyrssen and Wedborg (1991)
$Hg^{2+} + 2OH^- = Hg(OH)_2$	22.23	Dyrssen and Wedborg (1991)
$Hg^{2+} + 3OH^- = Hg(OH)_3^-$	20.9	Stumm and Morgan (1996)
$Hg^{2+} + Cl^- = HgCl^+$	7.2	Stumm and Morgan (1996)
$Hg^{2+} + 2Cl^- = HgCl_2$	14	Stumm and Morgan (1996)
$Hg^{2+} + 3Cl^- = HgCl_3^-$	15.1	Stumm and Morgan (1996)
$Hg^{2+} + 4Cl^- = HgCl_4^{2-}$	15.4	Stumm and Morgan (1996)
$Hg^{2+} + Cl^- + OH^- = HOHgCl$	18.1	Stumm and Morgan (1996)
$Hg^{2+} + OH^- + HS^- = HOHgSH$	40.51	Dyrssen and Wedborg (1991)
$Hg^{2+} + 2HS^- = Hg(SH)_2$	37.71	Schwarzenbach and Widmer (1963)
$Hg^{2+} + 2HS^- = HgS_2H^- + H^+$	31.53	Schwarzenbach and Widmer (1963)
$Hg^{2+} + 2HS^- = HgS_2^{2-} + 2H^+$	23.23	Schwarzenbach and Widmer (1963)
$Hg^{2+} + HS^- = HgS_s + H^+$	36.81	Schwarzenbach and Widmer (1963)
$Hg^{2+} + 2RS^- = Hg(SR)_2$	42	Skyllberg (2008)
$RS^- + H^+ = RSH$	10	Karlsson and Skyllberg (2003)
$H^+ + HS^- = H_2S$	7	Stumm and Morgan (1996)
$S_2^{2-} + H^+ = HS^-$	14.15	Schwarzenbach and Widmer (1963)
$H^+ + OH^- = H_2O$	13.7	

measured bulk-phase organic S : organic C ratio in the sediment of our study site (from data in Table 5; ~ 0.16 mol S mol^{-1} C; ~ 4.2 mass %) and the assumptions that the ratio of reduced organic S to total organic S concentration is ~ 20 mass % (Ravichandran 2004) and that the ratio of thiol to total reduced organic sulfur concentration is ~ 30 mass % (Qian et al. 2002). For example, a pore-water DOC concentration of 500 μmol L^{-1} (6 mg L^{-1}) would yield an estimated RSH concentration of ~ 0.47 μmol L^{-1} (15 μg L^{-1}). All speciation calculations were performed at 25°C, with a chloride concentration of 0.6 mol L^{-1} and an ionic strength of 0.5 mol L^{-1}.

Table 3. Dissolved organic carbon (DOC) concentrations in sediment pore water (0–4 cm) and overlying bottom water used for thermodynamic speciation modeling. Pore-water DOC concentrations were estimated on the basis of bulk organic carbon content, explained in more detail in Methods. Overlying water DOC concentrations were measured.

			DOC (μmol L^{-1})	
Month	Year	Site	Pore water	Bottom water
May	2005	6	515	109
Jul	2005	6	540	171
Sep	2005	6	520	137
Apr	2006	6	520	220
Jul	2006	6	508	233
Jul	2005	7	530	150
Sep	2005	7	520	137
Apr	2006	7	500	214
Jul	2006	7	499	154
Jul	2005	9	625	103
Sep	2005	9	650	77
Apr	2006	9	700	113
Jul	2006	9	799	138
Jul	2006	10	498	176
Jul	2006	12	989	102
Jul	2006	14	521	135

Calculation of inorganic Hg and MeHg diffusive fluxes—Diffusive fluxes (F) of dissolved Hg(II) and MeHg were calculated as described in Hollweg et al. 2009, using a diffusive transport equation on the basis of Fick's first law of diffusion.

The diffusive fluxes of MeHg and Hg(II) were determined by a summation of the fluxes of the individual MeHg and Hg(II) species present in solution (Eqs. 1 and 2). The MeHg species incorporated into the diffusive flux model include the following: $MeHgSH^0$, $MeHgS^-$, MeHgSR, and $MeHgCl^0$. The Hg(II) species incorporated into the diffusive flux model include the following: $HOHgSH^0$, HgS_2H^-, $HgS_2{}^{2-}$, $Hg(SR)_2$.

$$\sum F_{MeHg} = F_{MeHgSH^0} + F_{MeHgS^-} + F_{MeHgSR} + F_{MeHgCl^0} \quad (1)$$

$$\sum F_{Hg(II)} = F_{HOHgSH^0} + F_{HgS_2H^-} + F_{HgS_2{}^{2-}} + F_{Hg(SR)_2} \quad (2)$$

The diffusion coefficient at 25°C (D_w) of $HOHgSH^0$ was estimated to be 1.7×10^{-5} cm^2 s^{-1} on the basis of the inverse linear relationship between D_w and the molar volume (V) for neutrally charged molecules (Eq. 3: Hayduk and Laudie 1974; Schwarzenbach et al. 1993) and assuming the molar volume of 39 cm^3 mol^{-1} (Benoit et al. 2001*a*).

$$D_w = \left(\frac{2.3 \times 10^{-4}}{V^{0.71}}\right) \quad (3)$$

Using similar methods, the D_w of $MeHgSH^0$ and $MeHgCl^0$

Table 4. Average HgT and MeHg concentrations in sediment and pore water, sediment : water partition coefficients (K_D), and methylation (k_{meth}) and demethylation (k_{demeth}) rates in surface sediments (upper 4 cm) by station and cruise. Includes data collected from Sta. 6, 7, and 9 during May, July, and September 2005 and April 2006 (Hollweg et al. [2009]). Value listed is the average (± standard deviation) of duplicate or triplicate cores. Pore-water concentrations were single measurements. Slope stations designated (*).

		Sediment			Pore water			Log K_D				
Sampling date	Station	HgT (pmol g^{-1})	MeHg (pmol g^{-1})	% MeHg	HgT (pmol L^{-1})	MeHg (pmol L^{-1})	% MeHg	HgT (L kg^{-1})	MeHg (L kg^{-1})	k_{meth} (d^{-1})	k_{demeth} (d^{-1})	k_{meth} : k_{demeth}
May 2005	6	18.5±3.2	0.23±0.04	1.26±0.08	19.27	0.79	4.11	2.99	2.48	0.028±0.004	9.6±2.7	0.29
Jul 2005	6	16.4±1.1	0.17±0.00	1.07±0.08	11.84	1.24	10.46	3.16	2.15	0.011±0.003	3.2±2.7	0.33
Sep 2005	6	20.4±2.2	0.34±0.09	1.63±0.26	19.74	2.87	14.52	3.01	2.07	0.046±0.007	4.0±1.5	1.15
Apr 2006	6	17.5±1.3	0.21±0.05	1.23±0.37	20.32	1.60	7.89	2.95	2.12	0.025±0.008	2.0±3.0	1.25
Jul 2006	6	12.6±2.5	0.12±0.01	0.86±0.05	12.87	1.90	14.74	2.99	1.81	0.009±0.004	1.1±0.1	0.79
Jul 2005	7	46.2±5.3	0.62±0.10	1.27±0.06	21.47	2.45	11.39	3.33	2.50	0.020±0.004	9.2±0.4	0.22
Sep 2005	7	42.4±6.5	0.39±0.08	0.93±0.16	19.55	1.21	6.20	3.34	2.56	0.046±0.004	5.9±1.3	0.78
Apr 2006	7	7.6±0.1	0.11±0.03	1.41±0.34	5.11	0.87	17.09	3.17	2.09	0.004±0.000	3.3±1.6	0.12
Jul 2006	7	7.1±1.0	0.05±0.01	0.73±0.21	5.11	0.43	8.38	3.14	2.09	0.002±0.000	2.6±1.9	0.09
Jul 2006	10	3.1±0.4	0.04±0.00	1.14±0.22	5.46	0.29	5.38	2.75	2.10	0.003±0.001	1.8±0.6	0.14
Jul 2006	13	13.1±1.9	0.14±0.04	1.03±0.14	12.83	1.26	9.86	3.01	2.05	0.015±0.003	2.1±0.5	0.71
Jul 2006	14	14.4±3.7	0.16±0.02	0.91±0.08	17.77	0.82	4.61	2.91	2.29	0.011±0.008	2.1±0.4	0.52
Jul 2006	15	17.4±3.0	0.23±0.09	1.50±0.31	14.51	—	—	3.08	—	0.016±0.009	1.6±0.7	1.00
Average shelf		18.2±12.6	0.22±0.16	1.15±0.26	14.3±6.1	1.31±0.8	9.55±4.3	3.06±0.2	2.19±0.2	0.018±0.015	3.7±2.8	0.57±0.4
Jul 2005	9*	332±31.8	3.21±0.19	0.97±0.15	21.11	0.19	0.90	4.22	4.16	0.025±0.006	6.4±1.1	0.40
Sep 2005	9*	245±15.3	4.17±1.4	1.72±0.70	12.80	0.68	5.31	4.29	3.80	0.053±0.015	—	—
Apr 2006	9*	344±2.5	3.70±0.2	1.08±0.05	16.21	1.20	7.42	4.34	3.49	0.027±0.003	—	—
Jul 2006	9*	253±23.2	2.21±0.31	0.87±0.08	7.90	0.85	10.81	4.51	3.41	0.011±0.001	1.1±0.4	1.02
Jul 2006	9A*	34.6±4.2	0.41±0.07	1.18±0.21	19.67	6.61	33.63	3.25	1.79	0.021±0.002	1.3±0.1	1.57
Jul 2006	9B*	75.5±11.8	0.66±0.03	0.89±0.08	21.13	3.57	16.90	3.55	2.26	0.012±0.003	1.7±1.1	0.69
Jul 2006	11*	64.0±5.7	0.47±0.23	0.70±0.30	42.64	5.19	12.18	3.18	1.95	—	0.4±0.2	—
Jul 2006	12*	339±53.6	4.80±0.12	1.41±0.07	11.80	0.83	7.06	4.46	3.76	0.015±0.003	1.9±0.8	0.80
Average slope		210.9±132.4	2.45±1.77	1.1±0.33	19.16±10.6	2.39±2.4	11.78±10.0	3.97±0.6	3.08±0.9	0.023±0.014	2.1±2.2	0.9±0.44

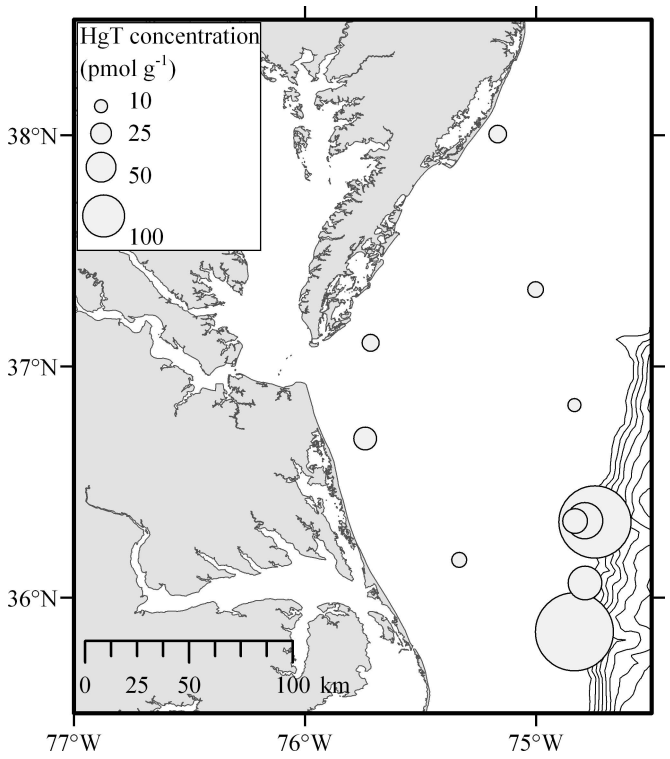

Fig. 2. Average bulk-phase HgT concentrations (pmol g^{-1} dry weight) measured in sediments of the mid-Atlantic continental shelf. A larger circle indicates a higher Hg concentration (as indicated in the figure legend).

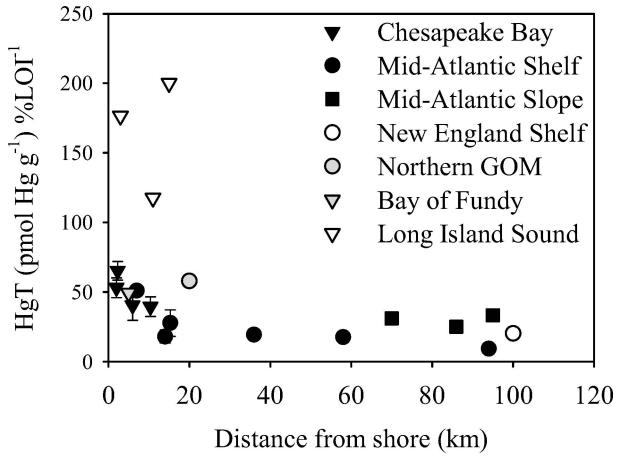

Fig. 3. Sediment HgT concentration, normalized to organic matter content (% loss on ignition), as a function of distance from shore for eastern North American coastal sediments. Black symbols represent data from this study and from Hollweg et al. (2009); error bars represent standard deviation between cruises for stations repeatedly sampled. Gulf of Mexico data from Liu et al. 2009; Long Island Sound from Hammerschmidt et al. 2004; New England Shelf from Hammerschmidt and Fitzgerald 2006; Bay of Fundy from Sunderland et al. 2006.

was assumed to be 1.2×10^{-5} cm^2 s^{-1} (Hammerschmidt et al. 2004) and 1.3×10^{-5} cm^2 s^{-1} (Gill et al. 1999), respectively. The D_w of MeHgSR and $Hg(SR)_2$ was assumed to be 2×10^{-6} cm^2 s^{-1} on the basis of the diffusion coefficient of organic matter (5000 Da) (Gill et al. 1999). The D_w of HgS_2^{-2} was assumed to be 9.5×10^{-6} cm^2 s^{-1} on the basis of the average diffusion coefficient of other doubly charged anionic species of similar mass (Li and Gregory 1974; Gill et al. 1999). The D_w of HgS_2H^- and $MeHgS^-$ was assumed to be 8.0×10^{-6} cm^2 s^{-1} on the basis of the average diffusion coefficient of other singly charged anionic species of similar mass (Li and Gregory 1974; Boudreau 1997; Goulet et al. 2007). Temperature corrections to the D_w were applied by the Stokes–Einstein equation, as discussed in Warnken et al. (2000).

Results

Spatial variations in concentration and partitioning of Hg and MeHg—Across the stations sampled (Fig. 1), HgT concentrations averaged around 20 pmol g^{-1} (dry weight) in sandy shelf sediments, and about 200 pmol g^{-1} in organic-rich slope sediments, with about an order of magnitude range in each (Table 4; Fig. 2). Sediment MeHg concentrations showed similar trends, with concentrations also about 10 times higher on the slope than on the shelf. For both bottom types, however, MeHg averaged about 1% of the HgT concentration. On the shelf, HgT concentrations were highest near the Chesapeake Bay mouth (Fig. 2; Table 4), where concentrations at Sta. 7 were about half those in sandy sediments of lower Chesapeake Bay (~ 70 pmol g^{-1}; Hollweg et al. 2009). Normalized to OM content, sediment HgT concentrations decreased with the distance offshore (Fig. 3).

Of the variables examined, bulk-phase HgT was the strongest correlate of MeHg in sediments (Fig. 4). This trend has been observed in many marine and freshwater systems, as discussed in Benoit et al. (2003). The slope of the linear relationship ($m = 0.012 \pm 0.001$) is equivalent to the average fraction of HgT that is MeHg (*see* %MeHg in Table 4). The average percentage of MeHg was similar to what was measured in deep-sea sediments of the Mediterranean Sea (Ogrinc et al. 2007), but at the higher end of the few other marine sediments that have been examined (Hammerschmidt and Fitzgerald 2006; Liu et al. 2009).

Pore-water HgT and MeHg concentrations varied much less than did bulk-phase concentrations, with interstitial water concentrations in slope sediments averaging only slightly higher than shelf sediments (Table 4). On average, MeHg made up 11% of HgT in interstitial waters. Pore-water Hg and MeHg concentrations were similar to those measured in the sediments of the nearby Chesapeake Bay (Benoit et al. 1998; Hollweg et al. 2009) and in other shelf sediments (Hammerschmidt and Fitzgerald 2006; Liu et al. 2009). Similar to bulk-phase Hg concentrations, the partitioning of Hg between the solid phase and pore water, defined as the distribution coefficient (K_D), varied by about two orders of magnitude, and was strongly correlated with OM content in sediments (Tables 4, 5).

Although MeHg concentrations in shelf and slope sediments were lower than in adjacent Chesapeake sediments, methylation rate constants, and the fraction of Hg as MeHg, were similar to or higher than in the estuary.

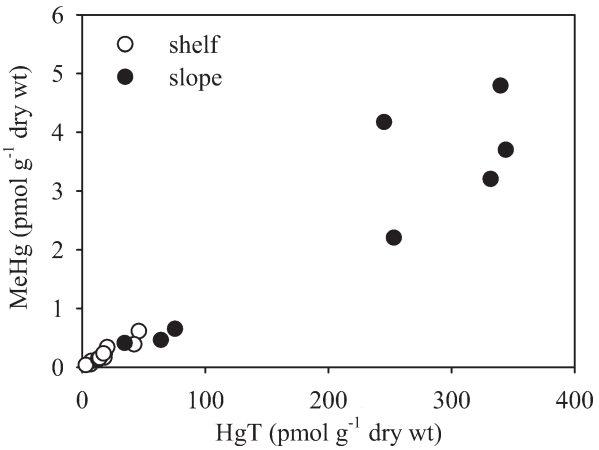

Fig. 4. Relationship between MeHg and HgT concentrations in surface sediments (0–4 cm). Each point represents the site average ($n = 2$ or 3) for an individual cruise. Graph includes data from all five cruises.

In mid-Atlantic shelf and slope surface (0–4 cm) sediments, we measured Hg methylation rate constants (k_{meth}) that ranged from about 0.002 to 0.05 d^{-1} (Table 4), similar to those measured with similar methods in the Chesapeake Bay (Heyes et al. 2006; Hollweg et al. 2009), New York–New Jersey Harbor (Hammerschmidt and Fitzgerald 2004), and other Atlantic estuaries (Heyes et al. 2006; Kim et al. 2006; Drott et al. 2008*a*). Demethylation rate constants (k_{demeth}) varied between 0.4 and 9.6 d^{-1}. To date, there have only been a handful of methylation rate studies in offshore sediments. The values estimated in this study were at the higher end of what was measured in deep-sea sediments of the Mediterranean Sea (Ogrinc et al. 2007) but at the lower end of what was measured on the southern New England continental shelf (Hammerschmidt and Fitzgerald 2006).

Discussion

The results suggest that the distribution of mercury across the study site is determined by sediment-binding capacity and proximity to sources. For MeHg, the redox zonation of sediments determines the depth distribution and magnitude of net MeHg production. Furthermore, the bioavailability of inorganic Hg for methylation appears to be the dominant driver of spatial patterns of MeHg across the shelf and slope. The relative importance of these factors is discussed in the following sections. Finally, the importance of the shelf and slope as a source of MeHg to the water column is estimated on the basis of diffusive calculations using measured concentrations of MeHg in pore water and overlying waters.

Controls on sediment Hg concentration—A strong association between Hg and organic matter has been observed in sediments of many marine ecosystems (Hammerschmidt and Fitzgerald 2004; Sunderland et al. 2006; Ogrinc et al. 2007). This interaction appears to be controlled by the strong association of Hg with thiol moieties in OM, as discussed in Ravichandran (2004) and Skyllberg (2008). In this study, sediment organic matter (SOM) explained more than 90% of the variability in Hg and MeHg concentrations (Fig. 5).

Table 5. Chemical characteristics of surface (0–4 cm) sediments (μmol g^{-1}) and pore waters (μmol L^{-1}) by station and cruise, including acid-volatile sulfide (AVS), chromium-reducible sulfide (CRS), and reactive Fe(II) and Fe(III).

Sampling date	Station	Sediment								Pore water			
		LOI (%)	C	S	N	AVS	CRS	Reac. Fe(II)	Reac. Fe(III)	pH	Sulfide	Fe	Mn
May 2005	6	0.92	—	—	—	1.35	10.97	—	—	8.13	0.24	17.51	11.65
Jul 2005	6	1.57	—	—	—	0.09	14.34	2.29	0.87	8.42	0.16	8.37	7.11
Sep 2005	6	1.07	—	—	—	0.55	9.66	3.97	0.48	7.79	0.38	32.54	15.66
Apr 2006	6	1.00	386	18.6	22.8	0.08	6.51	3.50	1.80	8.05	0.31	17.65	12.07
Jul 2006	6	0.55	—	—	—	0.28	9.19	3.71	0.82	7.30	0.15	11.55	5.21
Jul 2005	7	1.44	295	24.6	26.0	0.08	17.74	5.33	1.25	7.93	0.45	15.46	5.92
Sep 2005	7	1.09	365	26.5	32.3	0.98	29.41	5.63	0.69	7.84	0.88	35.94	6.91
Apr 2006	7	0.39	—	—	—	0.01	0.94	0.51	1.66	8.08	0.04	0.19	0.07
Jul 2006	7	0.35	—	—	—	0.00	1.28	0.72	2.02	7.52	0.01	0.33	0.77
Jul 2005	9*	8.70	2615	45.9	210.4	0.32	9.06	8.44	0.10	8.03	0.22	21.60	4.72
Sep 2005	9*	7.23	2754	47.1	207.3	0.36	24.55	7.13	0.01	7.56	1.16	24.21	4.64
Apr 2006	9*	10.92	3353	64.3	270.4	0.39	31.38	10.41	1.40	8.05	0.61	20.06	6.53
Jul 2006	9*	6.83	3167	79.3	240.7	0.02	8.60	9.13	0.18	7.59	0.05	1.29	0.90
Jul 2006	9A*	1.25	—	—	—	0.03	11.68	3.79	0.07	7.21	0.03	2.78	1.00
Jul 2006	9B*	2.41	1260	60.4	89.8	0.19	19.37	4.78	0.00	7.39	0.02	4.98	1.00
Jul 2006	10	0.33	—	—	—	0.01	1.68	0.21	0.60	6.95	0.03	0.55	0.04
Jul 2006	11*	2.55	1940	35.5	250.3	0.04	11.07	5.53	2.86	7.40	0.01	4.84	2.66
Jul 2006	12*	10.92	3687	93.4	720.7	1.55	22.33	18.27	0.00	7.60	0.08	39.06	8.97
Jul 2006	13	0.68	—	—	—	0.23	7.69	2.45	0.94	7.66	0.03	6.55	1.62
Jul 2006	14	0.82	—	—	—	0.31	5.00	1.45	1.54	7.10	0.07	6.66	4.86
Jul 2006	15	0.34	—	—	—	0.24	11.71	1.42	0.89	7.50	0.07	29.76	25.28

* Slope station.

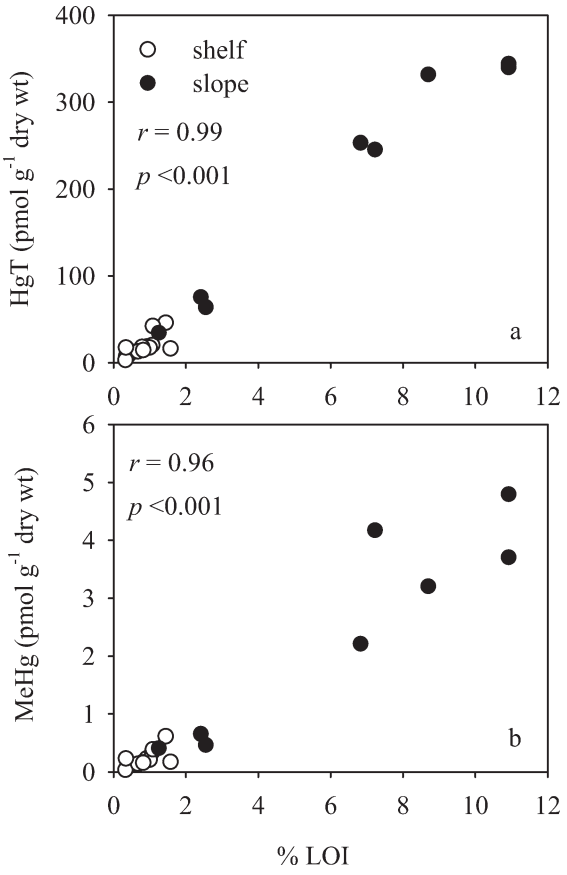

Fig. 5. (a) Total Hg and (b) MeHg concentrations in surface sediments (0–4 cm) plotted against organic matter content (as % LOI). Each point represents the site average (n = 2 or 3) for an individual cruise. Graph includes data from all five cruises.

Total Hg concentrations normalized to SOM content may be used as an indicator of relative contamination. In general, sediment Hg contamination decreases with distance from shore and thus from local point and nonpoint inputs. For example, Fig. 3 shows how SOM-normalized Hg concentrations decrease with distance from shore in our mid-Atlantic data set. Normalized to SOM, Chesapeake Bay sediments are somewhat less contaminated than those in Long Island Sound. Mid-Atlantic and coastal New England shelf sediments appear similarly contaminated, although somewhat less contaminated than sediments in the northern Gulf of Mexico. However, both distance from sources and changes in the chemistry of SOM with aging could contribute to these trends. For example, sediment organic S : C ratios decrease with distance offshore on the mid-Atlantic shelf (Hollweg et al. 2009), which could result in decreased Hg binding capacity. Additionally, the S : C ratio of Baltimore Harbor sediments ($\sim$ 0.1) is even higher than that of the Chesapeake Bay (Mason et al. 1999).

Organic matter controls on Hg partitioning—SOM also strongly influences Hg and MeHg partitioning behavior (Fig. 6; Eqs. 4, 5), and thus Hg availability for methylation, and MeHg availability for efflux and bioaccumulation. For the mid-Atlantic shelf and slope, we found the following relationships between SOM and sediment : water distribution coefficients:

$$\text{Log } K_D(\text{HgT}) = (2.97 \pm 0.06) + (0.15 \pm 0.02)[\%\text{LOI}] \quad (r = 0.94,\ p < 0.001,\ n = 22) \tag{4}$$

$$\text{Log } K_D(\text{MeHg}) = (1.98 \pm 0.09) + (0.18 \pm 0.02)[\%\text{LOI}] \quad (r = 0.90,\ p < 0.001,\ n = 22) \tag{5}$$

As observed in other systems, the slopes of the two linear regressions were parallel, with about an order of magnitude shift in the intercept.

As shown in Fig. 6, the relationship between SOM and Hg distribution coefficients varies across and within ecosystems, suggesting that the ability of sediments to bind Hg changes with source and age of SOM. The K_D is also related to the organic and inorganic S content of these sediments. More generally, the comparison across systems shows that the slope of the relationship declines with increasing SOM, particularly above about 5% LOI. Across a wide range of SOM, these relationships are better fit with log : log regressions. Overall, the HgT K_D appears to be higher in nearshore or more contaminated systems like New York Harbor, than in offshore or less affected sediments.

Biogeochemical controls on Hg methylation and MeHg demethylation—MeHg production rates in shelf and slope sediments were similar to or higher than sediment methylation rates in the adjacent Chesapeake Bay (Hollweg et al. 2009), despite the fact that offshore sediments support substantially lower rates of microbial activity. Average sulfate reduction and CO_2 production rates measured in shelf and slope surface sediments were about an order of magnitude lower than those measured in mid-bay sediments (Hollweg et al. 2009). This suggests that microbial activity is not the dominant control on net MeHg production, at least across broad spatial scales. Rather, sulfide and organic matter—parameters that influence Hg partitioning and bioavailability—were better predictors of methylation rates and %MeHg across the bay to slope transect (Hollweg et al. 2009).

The sandy sediments of the mid-Atlantic shelf and the clay sediments of the slope are mildly reducing environments, with low dissolved (< 10 μmol L^{-1}) and solid-phase (AVS + CRS) sulfide concentrations (Table 5). Low rates of carbon input yield low sediment oxygen demand, which, in combination with high porosity (in sand) and excess Fe (on the slope), result in low amounts of sulfide accumulation. However, the sediments are sufficiently reduced to support microbial sulfate reduction and probably Fe(III) reduction. Depth profiles of shelf and slope sediments generally showed a peak in k_{meth} in concert with a peak in dissolved Fe, usually within a few centimeters of the sediment surface (Hollweg et al. 2009).

Profiles of biogeochemical processes in shelf and slope sediments (Hollweg et al. 2009) showed that microbial sulfate reduction (SRR) accounted for roughly 5–10% of total CO_2 production during spring and 40–90% during

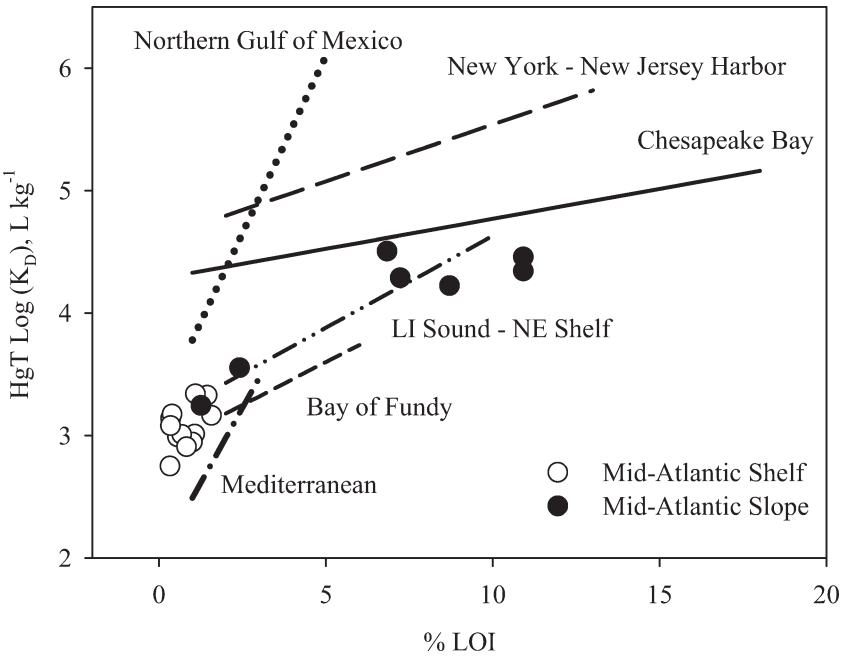

Fig. 6. Relationships between HgT sediment–water partition coefficients and sediment organic matter content (as % LOI) for a number of coastal ecosystems. Data points are from this study; each represents the site average (n = 2 or 3) for 0–4-cm depth sediment for an individual cruise. Lines are published relationships from other coastal areas: Chesapeake Bay (Hollweg et al. 2009), Long Island Sound and New England Shelf (Hammerschmidt and Fitzgerald 2006), northern Gulf of Mexico (Liu et al. 2009), Bay of Fundy (Sunderland et al. 2006), Mediterranean Sea (Ogrinc et al. 2007).

summer and fall in the upper 4 cm of the sandy sediment of the shelf (Sta. 6 and 7). In the organic-rich sediments of the slope (Sta. 9), SRR accounted for 60–100% of total CO_2 production in the upper 4 cm. Methane production was rarely detected even at depth (up to 12 cm) in shelf and slope sediments. Although we did not measure Fe(III) reduction rates directly, reactive Fe(III) was generally detectable in shelf surface sediments, and reactive Fe(II) was in excess of AVS, conditions that should support active Fe(II)-Fe(III) redox cycling.

On the shelf and slope, and in the Chesapeake, methylation was favored in sediment horizons that were reduced and supported microbial sulfate reduction, but were also low in dissolved sulfide, which is a strong inhibitor of MeHg production at concentrations above about 10 μmol L^{-1} (Gilmour et al. 1998; Hammerschmidt et al. 2008; Han et al. 2008). In organic, productive Chesapeake Bay sediments, that translates to a very narrow depth horizon near the sediment surface (Hollweg et al. 2009), limiting the depth-integrated amount of MeHg production. However, MeHg production in shelf and slope sediments occurs throughout a wide depth horizon.

In the mildly reduced surface sediments of the shelf and slope, methylation rates were positively correlated with biogeochemical indicators of reducing conditions, including pore-water Fe and sulfide, and sediment Fe(II) and AVS + CRS (Fig. 7), but not with microbial sulfate reduction rates. These relationships support the paradigm that Hg methylation is highest in low-oxygen, low-sulfide sediment, where reactive Fe is predominantly Fe(II) and dissolved sulfide is present at very low concentrations (0.1–1 μmol L^{-1}).

A positive correlation between pore-water sulfide and methylation rate in sediments or soils has rarely been observed, and only in systems with very low sulfide concentrations in interstitial water. Benoit et al. (1999, 2003) hypothesized that sulfide inhibits MeHg production through the formation of negatively charged Hg-S complexes that are poorly taken up by methylating bacteria. These complexes are favored as sulfide concentrations rise above about 10 μmol L^{-1} in most ecosystems. Benoit et al. (2001*a*) showed that microbial methylation rates are maximal at sulfide concentrations that favor the formation of neutrally charged Hg-S complexes, which generally occurs in the 0.1–10 μmol L^{-1} sulfide range.

In these coastal sediments, the positive relationship between sulfide and k_{meth} could be driven by the correlation between sulfide and microbial sulfate reduction activity, or the effect of sulfide on Hg partitioning, complexation, and bioavailability. Mercury methylation rates increased with total pore-water Hg concentration (Fig. 8a). In the sulfide concentration range observed, modeled Hg(II) speciation at all sulfide concentrations was dominated by neutrally charged Hg-S complexes (primarily HOHgSH and to a lesser extent $Hg(SH)_2$; here referred to as ΣHg-S^0), as illustrated by the similarity between Fig. 8a,b. Strong relationships between methylation rate and ΣHg-S^0 have been observed in other estuarine and marine systems (Drott

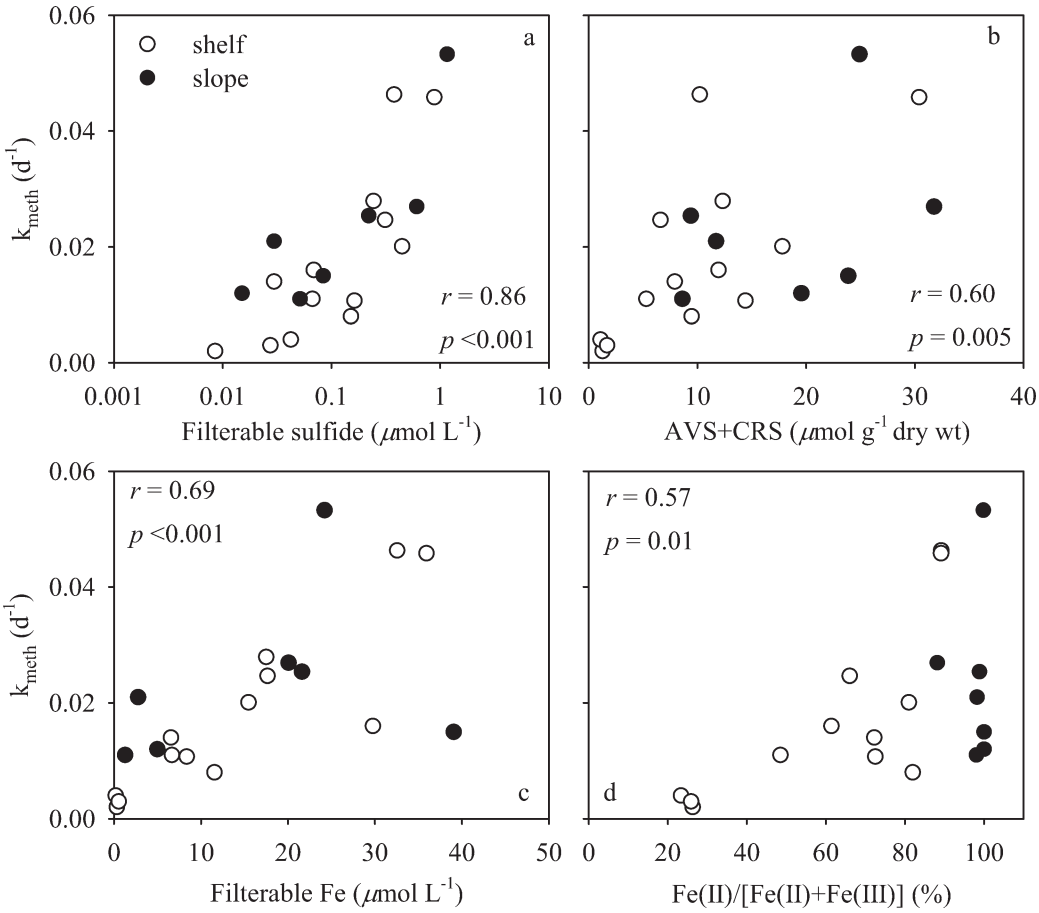

Fig. 7. Relationships between the methylation rate constant (k_{meth}) and biogeochemical parameters that may influence Hg bioavailability: (a) filterable sulfide; (b) sediment acid–volatile sulfide and chromium-reducible sulfide; (c) the filterable Fe concentration; and (d) the percentage of total sediment Fe as reactive Fe(II). Each point represents the site average (n = 2 or 3) for an individual cruise. Graph includes data from all five cruises.

et al. 2007), and methylation rates are correlated with total pore-water Hg concentration in marine sediments with very low dissolved sulfide concentrations (< 10 μmol L^{-1}; Hammerschmidt and Fitzgerald 2004, 2006).

Dissolved organic matter may also affect methylation through the formation of poorly available complexes or by altering the partitioning of Hg to the solid phase. However, the interaction between OM and Hg in the presence of sulfide remains poorly understood. Recent laboratory work has demonstrated that DOM may be more important in Hg speciation in the presence of dissolved sulfide (Hsu-Kim and Sedlak 2005; Miller et al. 2007; Deonarine and Hsu-Kim 2009) than previously thought. Potential interactions involve hydrophobic partitioning of neutral Hg complexes into SOM or stabilization of colloidal Hg-S particles (or nanoparticles) by OM. Thermodynamic speciation modeling of Hg in the presence of OM and sulfide is strongly dependent on the choice of stability constant, as the reported stability constants for the $Hg(SR)_2$ complex vary by many orders of magnitude (Ravichandran 2004; Skyllberg 2008). Here, we modeled the Hg-OM interaction as Hg bound to two reduced thiol groups, $Hg(SR)_2$, with a log K of 42 as suggested by Skyllberg (2008). Using this constant, the model yields < 2% of dissolved Hg as $Hg(SR)_2$ across all sites. We will explore dissolved Hg(II) speciation in more detail in another manuscript, across larger sulfide and OM gradients, including the comparison of the modeled bioavailable Hg(II) concentration to measured methylation rates.

Iron also plays a role in the control of net methylation, through its control of dissolved sulfide, and perhaps through other mechanisms. Methylation rates were correlated with both the pore-water Fe concentration and the redox status of reactive extractable Fe in sediments (Fig. 7). Although these trends are indicators of sediment redox status, we cannot rule out the role of Fe-reducing bacteria in Hg methylation. We did not directly measure Fe(III) reduction rates, but the observed biogeochemical conditions should support active iron reduction. Iron can also affect Hg mobility in sediment. For example, the dissolution of Fe(III) oxides has been observed to increase the pore-water concentration of Hg (Gobeil and Cossa 1993; Gagnon et al. 1996; Laurier et al. 2003), which in turn could increase Hg bioavailability to methylating bacteria. This could be another explanation for the observed relationship in Fig. 7, with an increase in methylation related to a release of adsorbed Hg into solution. However, although a positive relationship exists between Hg(II) K_D

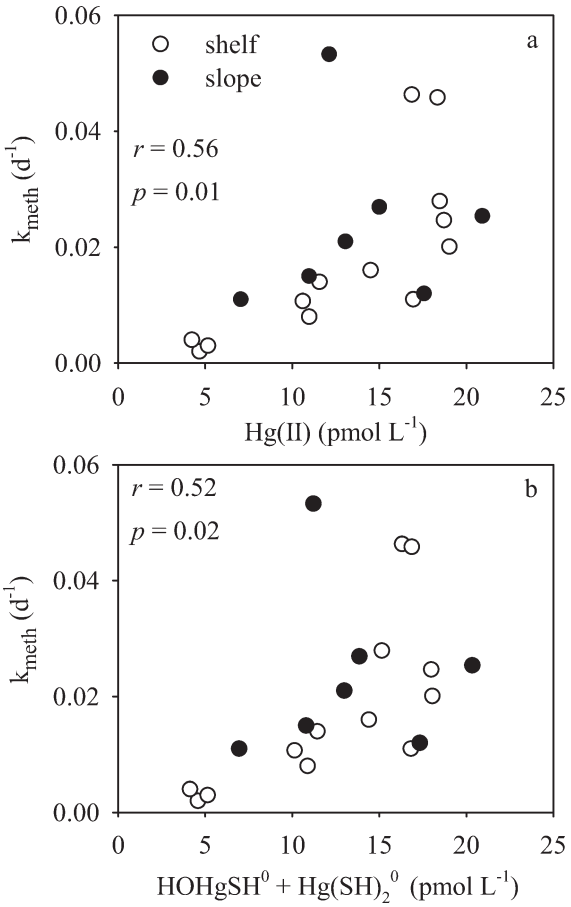

Fig. 8. Relationships between the methylation rate constant (k_{meth}) and Hg complexes in pore water. Mercury speciation was modeled as described. (a) Total filterable Hg(II); (b) neutral thiols and HOHgSH and $Hg(SH)_2$. Filterable Hg(II) speciation is dominated by the HOHgSH complex, explaining the similarity between the panels. Each point represents the site average (n = 2 or 3) for an individual cruise. Graph includes data from all five cruises.

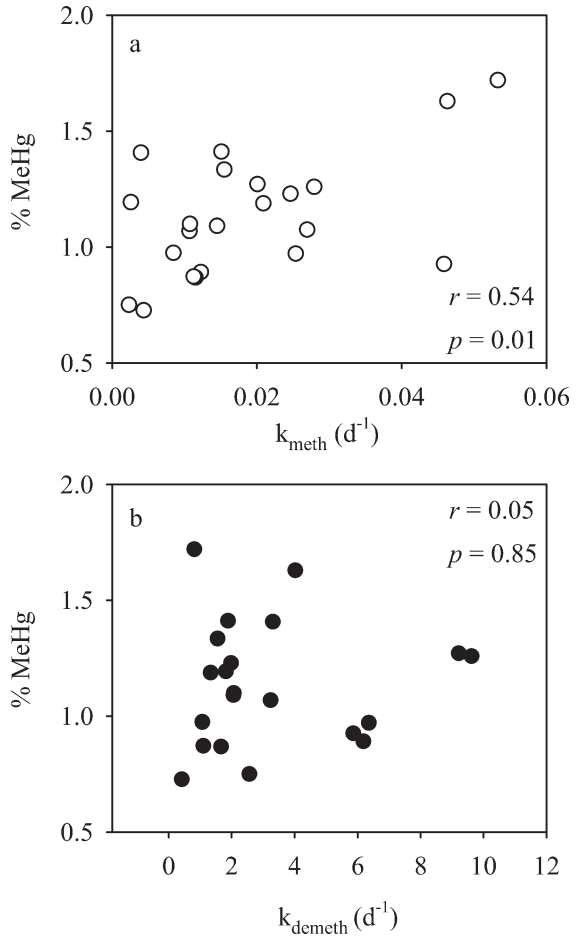

Fig. 9. Relationships between (a) the methylation and (b) demethylation rate constants and the percentage of total Hg as MeHg (% MeHg) in surface sediments (0–4 cm). Each point represents the site average (n = 2 or 3) for an individual cruise. Graph includes data from all five cruises.

and Fe(II)/[Fe(II)+Fe(III)] (r = 0.70, p = 0.016), this is most likely driven by the high covariation of Fe(II) and organic matter (r = 0.98, $p < 0.001$). Furthermore, the K_D normalized to OM (K_{OC}) was not significantly related to Fe redox chemistry ($p > 0.05$). Together, this indicates that Fe was not important in Hg mobility in the sediments of our study site, but was a secondary control, and reemphasizes that the partitioning of Hg between the solid phase and pore water was most strongly controlled by the OM content.

We also measured demethylation rates; however, they were not significantly correlated with %MeHg in sediments (Fig. 9), whereas methylation rates were. This has been observed in many other studies (Benoit et al. 2003; Drott et al. 2008*a*) and suggests that net MeHg production in most ecosystems is driven by the controls on its production rather than its degradation. Demethylation here can probably be attributed to the microbial pathway called "oxidative demethylation" (Oremland et al. 1991) since this, rather than the Hg-inducible *mer* operon-driven pathways, appears to be the dominant microbial demethylation process in uncontaminated or moderately contaminated sediments (Marvin-Dipasquale et al. 2000).

Like the Hg(II) methylation process, demethylation rates may depend upon the bioavailability of MeHg complexes to demethylating bacteria (Drott et al. 2008*b*). For shelf and slope sediments, the biogeochemical factors that correlated well with demethylation were similar to those that related to Hg methylation. The demethylation rate constants (k_{demeth}) increased significantly with dissolved sulfide concentration (Fig. 10), and with pH (data not shown, pH vs. k_{demeth}: p = 0.008, r = 0.58), but unlike methylation, demethylation was not related to dissolved or solid-phase Fe chemistry. Demethylation rates were inversely related to the modeled percentage of MeHg bound to organic matter ($MeHgSR^0$) (Fig. 11), suggesting that organically-bound MeHg is poorly bioavailable to demethylators. This is consistent with observations by Drott et al. (2008*b*) in freshwater sediments. Unlike methylation, the modeled concentration of the neutral $MeHgSH^0$ complex was not a good predictor of the demethylation rate. In fact, demethylation rates were better related to the

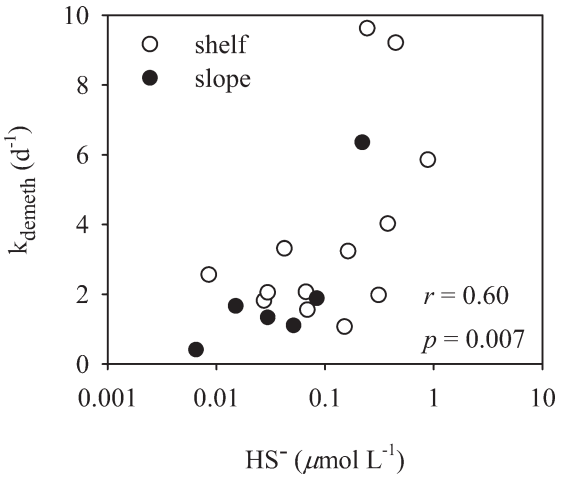

Fig. 10. Relationship between the demethylation rate constant (k_{demeth}) and the filterable sulfide concentration in surface sediments (0–4 cm). Each point represents the site average (n = 2 or 3) for an individual cruise.

modeled concentration of the negatively charged complex, $MeHgS^-$ (Fig. 11). However, the pK_a of the dissociation reaction of $MeHgSH^0$ ($MeHgSH^0 = MeHgS^- + H^+$; pK_a = 7.5) is near the average pH of coastal sediments. The balance between inorganic MeHg-S species and organic MeHg species (modeled as $MeHgSR^0$) is also sensitive to sulfide concentration in the range observed. Although one might reasonably expect the speciation of bioavailable MeHg to be similar to that of inorganic Hg, the uptake mechanisms for MeHg by oxidative demethylators are unknown, and the species favored for demethylation are not well understood. Demethylation has been found to be relatively ubiquitous across ecosystems, and it occurs both in oxic and anoxic environments, so it is possible that uptake is due to a facilitated process rather than purely due to passive uptake. In such a case, it is possible that the labile fraction (i.e., the total fraction as inorganic complexes) is a better proxy for uptake bioavailability than is the neutral complex concentration, as it is for other metals that are actively assimilated (e.g., Fe, Zn) (Morel and Hering 1993). The positive correlation in Fig. 11 suggests that uptake is related to the concentration of small, labile MeHg complexes.

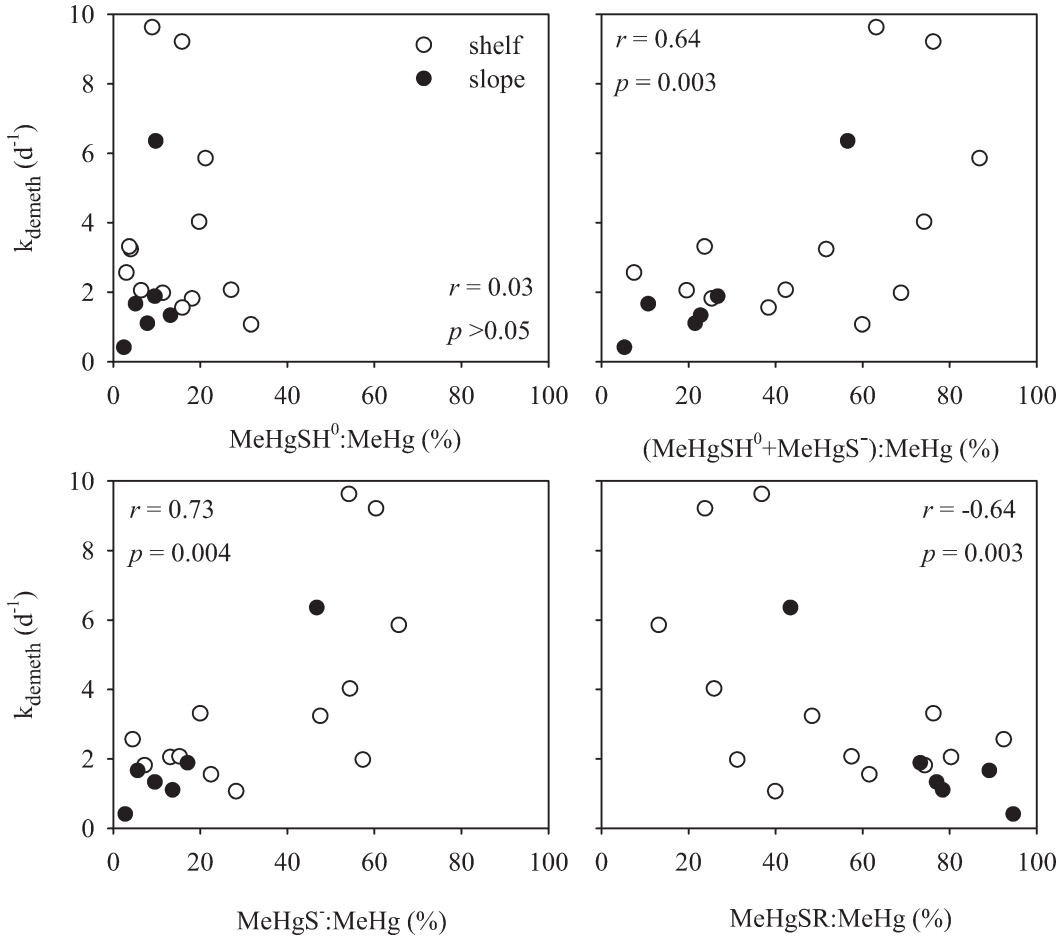

Fig. 11. Relationships between the demethylation rate constant (k_{demeth}) and MeHg speciation as a fraction of total filterable MeHg in pore water. MeHg speciation was modeled as described. Each point represents the site average (n = 2 or 3) for 0–4-cm depth sediment for an individual cruise.

Diffusive flux estimates—Mercury and MeHg concentrations in surficial sediment pore waters exceeded concentrations in surface waters at all sites on all sampling dates (Tables 6 and 7). Thus, on the basis of Fick's Law of Diffusion, all sites were sources of Hg(II) and MeHg to the water column. Diffusive flux rates were estimated by modeling the equilibrium speciation of dissolved complexes, applying separate diffusion coefficients for each complex, and summing the individual fluxes (*see* Methods). Using this approach, the calculated diffusive flux of MeHg ranged from 0.05 to 2.2 pmol m^{-2} d^{-1} (Table 7), with an average flux of 0.8 pmol m^{-2} d^{-1}. The variation in the flux across sites was strongly related to the modeled speciation of MeHg in the pore water and the associated diffusion coefficient (D_w) for that complex. Dissolved sulfide concentrations were clearly important in controlling the flux. For example, in sediments where the MeHg-S complexes ($MeHgSH^0$ and $MeHgS^-$) dominated, the overall diffusive flux was significantly higher than for sediments where the organically bound MeHg complex ($MeHgSR^0$) dominated, due to an order of magnitude higher D_w for MeHg bound to sulfide than bound to OM. The diffusive flux of MeHg would therefore be significantly higher from more reducing sediments with shallower oxygen penetration, as this would result in a higher proportion of MeHg-S species near the surface of the sediment. Seasonal changes in pore-water sulfide, and thus MeHg-S concentrations, in surface pore water explain the seasonal variations in the calculated MeHg diffusive flux at individual stations (Table 7).

For Hg(II), the calculated diffusive flux ranged from 3.4 to 60 pmol m^{-2} d^{-1} (Table 6), with an average flux of 26 pmol m^{-2} d^{-1}. The variations in flux between sites were primarily controlled by differences in pore-water Hg(II) concentrations, since modeled Hg complexation did not vary substantially across sites. However, it should be noted that the diffusive flux of Hg(II) may be potentially overestimated, as recent work has shown a significant interaction between dissolved Hg(II) and DOM in the presence of sulfide (Hsu-Kim and Sedlak 2005; Miller et al. 2007; Deonarine and Hsu-Kim 2009), which thermodynamic models do not accurately predict.

In contrast to most published flux estimates that have used the simplifying assumption that Hg speciation is the same in surface and pore water, we modeled the speciation in both separately and used the concentration differences for each species in generating the flux estimates. These speciation differences can have a large effect on the estimated diffusive flux. As shown in Table 6, there were instances where a negative flux of $Hg(SR)_2$ occurred because of a higher concentration of $Hg(SR)_2$ in the overlying water relative to the pore water. In most instances, the Hg and MeHg sulfide complexes had the highest calculated flux rates because of the high diffusion coefficients and the low concentrations of Hg-S complexes in the overlying water.

The MeHg and Hg(II) diffusive fluxes estimated in this study were at the lower range of those calculated for the southern New England continental shelf (Hammerschmidt and Fitzgerald 2006), Mediterranean Sea (Ogrinc et al. 2007), San Francisco Bay (Choe et al. 2004), Boston Harbor

Table 6. Concentrations and diffusive fluxes of dissolved Hg(II) species estimated in pore water and bottom water of the study site, separated by station and cruise. The diffusive flux rates were estimated by applying separate diffusion coefficients for each complex, and summing the individual fluxes.

Sampling date	Station	Hg(II) Concentration (pmol L^{-1})										Flux (pmol m^{-2} d^{-1})					
		Pore water						Bottom water									
		HOHgSH	$Hg(SR)_2$	$Hg(SH)_2$	HgS_2H^{-1}	HgS_2^{2-}	HOHgSH	$Hg(SR)_2$	$Hg(SH)_2$	HgS_2H^{-1}	HgS_2^{2-}	HoHgSH	$Hg(SR)_2$	HgS_2H^{-1}	HgS_2^{2-}	Sum
May 2005	6	15.14	0.06	0.00	0.20	3.08	0.00	6.41	0.00	0.00	0.00	21.43	−1.05	0.13	2.42	22.93
Jul 2005	6	10.13	0.08	0.00	0.08	0.31	0.00	4.91	0.00	0.00	0.00	15.51	−0.86	0.06	0.26	14.97
Sep 2005	6	16.31	0.01	0.01	0.29	0.25	0.00	7.59	0.00	0.00	0.00	30.30	−1.65	0.25	0.26	29.17
Apr 2006	6	17.98	0.03	0.00	0.27	0.42	0.00	2.91	0.00	0.00	0.00	22.68	−0.42	0.16	0.30	22.72
Jul 2006	6	10.88	0.01	0.00	0.06	0.02	0.00	5.03	0.00	0.00	0.00	20.54	−1.11	0.06	0.02	19.51
Jul 2005	7	18.04	0.02	0.00	0.41	0.54	0.00	3.45	0.00	0.00	0.00	23.71	−0.53	0.25	0.40	23.83
Sep 2005	7	16.85	0.01	0.01	0.74	0.73	0.00	8.20	0.00	0.00	0.00	26.69	−1.52	0.55	0.64	26.36
Apr 2006	7	4.12	0.09	0.00	0.01	0.02	0.00	5.86	0.00	0.00	0.00	4.01	−0.66	0.00	0.01	3.37
Jul 2006	7	4.59	0.09	0.00	0.00	0.00	0.00	1.66	0.00	0.00	0.00	6.16	−0.25	0.00	0.00	5.91
Jul 2005	9	20.34	0.06	0.00	0.21	0.30	0.00	6.08	0.00	0.00	0.00	51.16	−1.77	0.24	0.43	50.06
Sep 2005	9	11.20	0.00	0.02	0.60	0.30	0.00	1.28	0.00	0.00	0.00	31.56	−0.42	0.79	0.48	32.41
Apr 2006	9	13.85	0.03	0.00	0.43	0.69	0.00	5.79	0.00	0.00	0.00	59.37	−2.89	0.87	1.65	59.00
Jul 2006	9	6.95	0.07	0.00	0.02	0.01	0.00	0.73	0.00	0.00	0.00	27.95	−0.31	0.03	0.02	27.69
Jul 2006	10	5.15	0.01	0.00	0.00	0.00	0.00	2.66	0.00	0.00	0.00	4.23	−0.25	0.00	0.00	3.98
Jul 2006	12	10.80	0.10	0.00	0.04	0.02	0.00	14.10	0.00	0.00	0.00	55.20	−8.37	0.10	0.06	47.00
Jul 2006	14	16.81	0.03	0.00	0.04	0.07	0.00	5.59	0.00	0.00	0.00	32.70	−1.27	0.03	0.07	31.54

Table 7. Concentrations and diffusive fluxes of dissolved MeHg species estimated in pore water and bottom water of the study site, separated by station and cruise. The diffusive flux rates were estimated by applying separate diffusion coefficients for each complex, and summing the individual fluxes.

Sampling date	Station	MeHg concentration (pmol L^{-1})								Flux (pmol m^{-2} d^{-1})				
		Pore water				Bottom water								
		$MeHgS^-$	MeHgSH	MeHgSR	MeHgCl	$MeHgS^-$	MeHgSH	MeHgSR	MeHgCl	$MeHgS^-$	MeHgSH	MeHgSR	MeHgCl	Sum
May 2005	6	0.428	0.071	0.291	0.000	0.000	0.000	0.067	0.000	0.28	0.07	0.04	0.00	0.39
Jul 2005	6	0.590	0.050	0.600	0.000	0.000	0.000	0.082	0.000	0.42	0.05	0.09	0.00	0.57
Sep 2005	6	1.560	0.566	0.741	0.001	0.000	0.000	0.152	0.001	1.36	0.74	0.13	0.00	2.22
Apr 2006	6	0.918	0.183	0.499	0.000	0.000	0.000	0.063	0.000	0.54	0.16	0.06	0.00	0.77
Jul 2006	6	0.537	0.602	0.759	0.002	0.000	0.000	0.105	0.000	0.47	0.80	0.14	0.00	1.42
Jul 2005	7	1.480	0.388	0.583	0.000	0.000	0.000	0.237	0.000	0.91	0.36	0.05	0.00	1.32
Sep 2005	7	0.794	0.257	0.159	0.000	0.000	0.000	0.077	0.000	0.59	0.29	0.02	0.00	0.89
Apr 2006	7	0.174	0.032	0.664	0.000	0.000	0.000	0.042	0.000	0.08	0.02	0.07	0.00	0.17
Jul 2006	7	0.019	0.013	0.397	0.001	0.000	0.000	0.050	0.000	0.01	0.01	0.05	0.00	0.08
Jul 2005	9	0.089	0.019	0.083	0.000	0.000	0.000	0.050	0.000	0.10	0.03	0.01	0.00	0.15
Sep 2005	9	0.370	0.233	0.077	0.000	0.000	0.000	0.141	0.001	0.49	0.46	−0.02	0.00	0.93
Apr 2006	9	0.763	0.152	0.285	0.000	0.000	0.000	0.050	0.000	1.53	0.46	0.12	0.00	2.11
Jul 2006	9	0.116	0.067	0.666	0.001	0.000	0.000	0.259	0.001	0.22	0.19	0.19	0.00	0.60
Jul 2006	10	0.021	0.053	0.215	0.001	0.000	0.000	0.050	0.000	0.01	0.03	0.02	0.00	0.05
Jul 2006	12	0.142	0.080	0.608	0.000	0.000	0.000	0.383	0.012	0.34	0.29	0.13	−0.05	0.71
Jul 2006	14	0.125	0.222	0.471	0.002	0.000	0.000	0.050	0.000	0.11	0.30	0.10	0.00	0.51

(Benoit et al. 2009), and Chesapeake Bay (Hollweg et al. 2009), with similar methods, and more than an order of magnitude lower than those estimated at other sites (Mikac et al. 1999; Hammerschmidt and Fitzgerald 2008), as outlined in Table 8. The differences in flux estimations were primarily driven by differences in measured pore-water concentrations across sites, as the diffusive flux coefficients (D_w) used in these other studies were similar to or lower than what was used in this study. However, it is obvious that there are many inconsistencies within these diffusive flux calculations between studies, with variations in the values used for the coefficients such as D_w and Δx (the average depth of the pore-water sample).

To assess the role of the continental shelf and slope in the Hg(II) and MeHg ocean budgets, it is possible to integrate the calculated diffusive flux over the entire shelf area of the world's ocean. However, it should be noted that this is a minimum estimate of the flux from bottom sediments since measured fluxes are almost always substantially greater than the calculated diffusive flux (Table 8) because of other physical and biological processes, such as advection, bioturbation, bioirrigation, and resuspension (Schnoor 1996). Although no benthic flux measurements for Hg have been performed at our study area, similar conclusions have been reached for the flux of other compounds measured from the Atlantic continental shelf and slope. For example, the total measured DOC flux was $\sim 10\times$ higher than the calculated diffusive flux from the permeable sediments in the mouth of Chesapeake Bay (Burdige et al. 2004), the measured $Si(OH)_2$ and NH_4^+ fluxes were, on average, $\sim 30\times$ higher than the calculated diffusive fluxes from sediments on the southern Atlantic Bight (Jahnke et al. 2005), and the measured dissolved inorganic carbon flux was $\sim 2\times$ higher than the calculated diffusive flux from sediments on the mid-Atlantic continental slope (Thomas et al. 2002). In Boston Harbor sediments, MeHg fluxes measured in core incubations were roughly an order of magnitude higher than calculated diffusive fluxes, and were directly related to the density of benthic infauna (Benoit et al. 2009).

Using the area of the shelf and slope above 1000-m depth (3.5×10^{13} m^2; calculated with MATLAB mathematical computing software), the diffusive inputs of Hg(II) and MeHg from the sediments of the shelf and slope to the coastal ocean would be 0.37 and 0.01 Mmol yr^{-1}, respectively. The calculated area is $\sim 10\%$ of the total area of the world's oceans ($\sim 3.5 \times 10^{14}$ m^2). The flux estimate for total Hg is similar to that of Cossa et al. (1996), who estimated the input at 0.5 Mmol yr^{-1} for the coastal zone (estimated as 10% of the total sedimentary input). For MeHg, the authors derived a much lower value, but these earlier estimates were based on limited knowledge of the concentrations of MeHg in shelf sediment pore waters and overlying waters.

For the Hg(II) budget, the diffusive input is small relative to other loading terms to the shelf, such as riverine input (~ 2.9 Mmol yr^{-1}; Sunderland and Mason 2007) and wet plus dry atmospheric deposition (1.5–3 Mmol yr^{-1}). The deposition estimate is based on 10–20% of the total Hg load in Mason and Sheu (15.4 Mmol yr^{-1}; 2002), given that

Table 8. Comparison of the estimated HgT and MeHg diffusive fluxes in the mid-Atlantic continental shelf to those determined for other marine and estuarine regions (Gobeil and Cossa 1993; Gagnon et al. 1997; Covelli et al. 1999; Gill et al. 1999; Mikac et al. 1999; Choe et al. 2004; Hammerschmidt et al. 2004; Hammerschmidt and Fitzgerald 2006*b*; Muresan et al. 2007; Ogrinc et al. 2007; Point et al. 2007; Covelli et al. 2008; Hammerschmidt et al. 2008; Rothenberg et al. 2008; Benoit et al. 2009; Hollweg et al. 2009). The assumptions used in the calculations are listed, including the diffusion coefficient at 25°C (D_w), the modeled complex, and the average depth of the pore-water sample (Δx). In addition, the measured flux (using benthic chambers or intact sediment core incubation experiments) and the ratio of the measured flux to the diffusive flux are listed.

	Calculated diffusive flux (pmol m^{-2} d^{-1})					Measured flux (pmol m^{-2} d^{-1})			
	Range	Avg	D_w (cm^2 s^{-1}) at 25°C	Species	Depth (cm)	Range	Avg	Measured : calculated	Reference
Hg(II)									
Mid-Atlantic Cont. Shelf	3.4–60	26	2×10^{-6}–1.7×10^{-5}	HOHgSH, HgS_2H^-, HgS_2^{2-}, Hg-DOM	1	—	—	—	This study
Grado Lagoon*	−185–475	161	5×10^{-6}	—	0.5	29,500–166,000	77,933	482	Covelli et al. (2008)
Mugu Lagoon	−2.5–375	—	9.5×10^{-6}	$HgCl_4$	1	—	—	—	Rothenberg et al. (2008)
Mugu Lagoon	−0.5–80	—	2×10^{-6}	Hg-DOM	1	—	—	—	Rothenberg et al. (2008)
Mediterranean Sea	33–206	~105	9.5×10^{-6}	$HgCl_4$	1	—	—	—	Ogrinc et al. (2007)
Thau Lagoon	—	40	8.65×10^{-6} at 18°C	$HgCl_4$	0.5	−6800–2600	—	20	Point et al. (2007); Muresan et al. (2007)
San Fracisco Bay-Delta	1.3–220	44	5×10^{-6}	—	0.5	−1500–2600	629	4.2–500	Choe et al. (2004)
Gulf of Trieste	−10.6–206	55	5×10^{-6}	—	0.5	135–32,280	7976	9–1061	Covelli et al. (1999)
Lavaca Bay, Texas†	24–05	84	9.5×10^{-6}	$HgCl_4$	0.5	—	—	—	Gill et al. (1999)
Lavaca Bay, Texas†	2–85	18	2×10^{-6}	Hg-DOM	0.5	—	—	—	Gill et al. (1999)
Seine Estuary, France	5189–7921	—	5×10^{-6}	—	0.5	—	—	—	Mikac et al. (1999)
St. Lawrence Estuary	1229–3687	2253	5×10^{-6}	—	0.25	—	—	—	Gagnon et al. (1997)
Laurentian Trough	—	130	5×10^{-6}	—	1	—	—	—	Gobeil and Cossa (1993)
MeHg									
Mid-Atlantic Cont. Shelf	0.0–2.2	0.8	2×10^{-6}–1.3×10^{-5}	MeHgSH, $MeHgS^-$, MeHg-DOM, MeHgCl	1	—	—	—	This study
Boston Harbor	2–19	8.5	1.2×10^{-5}	MeHgSH	1	−4–191	75	5.5–38.2	Benoit et al. (2009)
Chesapeake Bay	−3.6–58	5.1	1.2×10^{-5}	MeHgSH	1	—	—	—	Hollweg et al. (2009)
Grado Lagoon*	−10–85	44	1.2×10^{-5}	MeHgSH	0.5	1050–7450	4000	91	Covelli et al. (2008)
NY NJ Harbor	13–86	46	1.2×10^{-5}	MeHgSH	1	39–92	64	1–4.3	Hammerschmidt and Fitzgerald (2008)
Mugu Lagoon	0.7–26.5	8.5	1.2×10^{-5}	MeHgSH	1	—	—	—	Rothenberg et al. (2008)
Mediterranean Sea	3–32	~18	1.3×10^{-5}	MeHgCl	1	—	—	—	Ogrinc et al. (2007)
Thau Lagoon		4	1.84×10^{-5} at 18°C	MeHgCl	0.5	−147–334	—	66	Point et al. (2007); Muresan et al. (2007)
SNE Cont. Shelf	6.6–12	9	1.2×10^{-5}	MeHgSH	1	—	—	—	Hammerschmidt and Fitzgerald (2006*b*)
San Fracisco Bay-Delta	−1.3–140	150	5×10^{-6}		0.5	−92–850	64	1.5–333	Choe et al. (2004)
Long Island Sound	12–174	75	1.2×10^{-5}	MeHgSH	1	—	—	—	Hammerschmidt et al. (2004)
Gulf of Trieste	−8.9–22	6.45	5×10^{-6}		0.5	−525–11,850	1894	11–300	Covelli et al. (1999)
Lavaca Bay, Texas†	2–200	65	1.3×10^{-5}	MeHgCl	0.5	75	—	1.25	Gill et al. (1999)
Lavaca Bay, Texas†	0.5–31	10	2×10^{-6}	MeHg-DOM	0.5	75	—	8	Gill et al. (1999)

* Open lagoon.
† Open water sites.

the Hg concentration in coastal rain is likely elevated compared with that of the open ocean. These inputs are similar to those estimated by Cossa et al. (1996), with riverine input at ~ 4.8 Mmol yr^{-1} and atmospheric deposition at ~ 2 Mmol yr^{-1}. In addition, the diffusive input is similar, but lower, than the estimated Hg sedimentation load to the shelf (1 Mmol yr^{-1}; Sunderland and Mason 2007).

For the MeHg budget, this minimum diffusive input is on the same order as other loadings to the shelf region, such as riverine input (0.029 Mmol yr^{-1}; assuming 1% MeHg in the riverine Hg input estimates of Sunderland and Mason [2007]) and atmospheric wet plus dry deposition (0.008–0.015 Mmol yr^{-1}, assuming 0.5% MeHg in deposition). These MeHg inputs are on the same order as those estimated by Cossa et al. (1996), with riverine input at ~ 0.01 Mmol yr^{-1} and atmospheric deposition at ~ 0.02 Mmol yr^{-1}. It could be argued that as the diffusive flux is roughly equivalent to the net sedimentation of MeHg (0.01 Mmol yr^{-1}, assuming 1% MeHg in settling particles and the Hg sedimentation flux in Sunderland and Mason 2007), there is no net production and export of MeHg from these sediments. However, if we assume that the diffusive input is underestimating the total MeHg load by an order of magnitude because of other physical and biological processes (discussed above), continental margin sediments, at ~ 0.1 Mmol yr^{-1}, become a major source of MeHg to the coastal zone. The ratio of actual flux to the calculated diffusive flux could be even higher, on the basis of the studies in Table 8. Additionally, given the estimated sedimentation input above, it is apparent that, on average globally, the shelf and slope sediments are a net source of MeHg to the ocean. This conclusion may not be valid for all regions. For example, the modeling study of Sunderland et al. (2010) actually reaches the opposite conclusion for the dynamic system of the Bay of Fundy, in which the sedimentary inputs from net in situ methylation are small compared with other MeHg sources.

As discussed in the introduction, water-column methylation may be another significant source of MeHg in coastal and open oceans, but remains poorly quantified. Most observations of Hg methylation or MeHg maxima in the marine water column have been associated with lower oxygen concentrations (Mason and Fitzgerald 1993; Kirk et al. 2008; Cossa et al. 2009) or depths below the photic zone in horizons of high organic carbon remineralization (Sunderland et al. 2009). These observations suggest that MeHg production in the shallow, well-mixed water column (< 20 m) of the shelf would be quite low. An exception is the observation of MeHg in coastal surface waters of the Mediterranean Sea (Monperrus et al. 2007*a*,*b*). However, Whalin et al. (2007) were unable to detect Hg methylation in mid-Atlantic continental shelf surface waters using stable isotope incubation experiments similar to those used by Monperrus et al. (2007*a*,*b*).

Our data show that shelf and slope sediments are areas of significant MeHg production and input to overlying waters. Rough budgets suggest that sediments are a major source of MeHg to the continental shelves, and likely an important source to blue waters. Direct flux measurements are required to further quantify the importance of sediments to coastal and marine MeHg budgets, as substantial physical and biological enhancement of the dissolved MeHg flux is likely. As this study refers to a specific marine system, we emphasize the need to expand this research across a larger spatial scale, and in other marine environments, to validate the preliminary scaling estimates presented above. We conclude that the overall cycling of MeHg across the sediment water interface, which also includes sedimentation and resuspension, needs to be considered in any estimation of the net input of MeHg from sediments to the water column.

Acknowledgments

We thank the captains and crews of the RV *Cape Henlopen*, RV *Hugh Sharp*, and RV *Cape Hatteras*; our colleague Marcelino Suzuki and the crew of the RVs *Henlopen* and *Sharp* for their successful efforts to modify an Ocean Instruments box corer for use in sand; Georgia Riedel, Tyler Bell, Evan Malczyk, Liz Kerin, and Genevieve Bernier for technical assistance in the field and lab; and James O'Donnell for help with MATLAB.

This work was supported by the National Science Foundation (NSF) 0351050 to R.P.M. and C.C.G.; and the SERC Research Experience for Undergraduates Program, by the Environmental Protection Agency STAR graduate fellowship and the William A. Lund, Jr., Fellowship to T.A.H., and by the Smithsonian Marine Sciences Network.

References

Alperin, M. J., C. S. Martens, D. B. Albert, I. B. Suayah, L. K. Benninger, N. E. Blair, and R. A. Jahnke. 1999. Benthic fluxes and pore-water concentration profiles of dissolved organic carbon in sediments from the North Carolina continental slope. Geochim. Cosmochim. Acta **63:** 427–448, doi:10.1016/S0016-7037(99)00032-0

Benoit, J. M., C. C. Gilmour, A. Heyes, R. P. Mason, and C. L. Miller. 2003. Geochemical and biological controls over methylmercury production and degradation in aquatic systems, p. 262–297. *In* Y. Cai and O. C. Braids [eds.], Biogeochemistry of environmentally important trace elements. ACS Symposium Series 835.

———, ———, and R. P. Mason. 2001*a*. The influence of sulfide on solid phase mercury bioavailability for methylation by pure cultures of *Desulfobulbus propionicus* (1pr3). Environ. Sci. Technol. **35:** 127–132, doi:10.1021/es001415n

———, ———, ———, and A. Heyes. 1999. Sulfide controls on mercury speciation and bioavailability to methylating bacteria in sediment pore waters. Environ. Sci. Technol. **33:** 951–957, doi:10.1021/es9808200

———, ———, ———, G. S. Riedel, and G. F. Riedel. 1998. Behavior of mercury in the Patuxent River estuary. Biogeochemistry **40:** 249–265, doi:10.1023/A:1005905700864

———, R. P. Mason, C. C. Gilmour, and G. R. Aiken. 2001*b*. Constants for mercury binding by dissolved organic matter isolates from the Florida Everglades. Geochim. Cosmochim. Acta **65:** 4445–4451, doi:10.1016/S0016-7037(01)00742-6

———, D. H. Shull, R. M. Harvey, and S. A. Beal. 2009. Effect of bioirrigation on sediment–water exchange of methylmercury in Boston Harbor, Massachusetts. Environ. Sci. Technol. **43:** 3669–3674, doi:10.1021/es803552q

Black, F. J., A. Paytan, K. L. Knee, N. R. De Sieyes, P. M. Ganguli, E. Gary, and A. R. Flegal. 2009. Submarine groundwater discharge of total mercury and monomethylmercury to Central California coastal waters. Environ. Sci. Technol. **43:** 5652–5659, doi:10.1021/es900539c

Boudreau, B. P. 1997. Diagenetic models and their implementation. Springer.

Burdige, D. J., and J. Homstead. 1994. Fluxes of dissolved organic-carbon from Chesapeake Bay sediments. Geochim. Cosmochim. Acta **58:** 3407–3424, doi:10.1016/0016-7037(94)90095-7

———, S. W. Kline, and W. H. Chen. 2004. Fluorescent dissolved organic matter in marine sediment pore waters. Mar. Chem. **89:** 289–311, doi:10.1016/j.marchem.2004.02.015

Choe, K. Y., G. A. Gill, R. D. Lehman, S. Han, W. A. Heim, and K. H. Coale. 2004. Sediment–water exchange of total mercury and monomethyl mercury in the San Francisco Bay delta. Limnol. Oceanogr. **49:** 1512–1527, doi:10.4319/lo.2004.49.5.1512

Cossa, D., M. Coquery, C. Gobeil, and J. M. Martin. 1996. Mercury fluxes at the ocean margin, p. 229–247. *In* W. Baeyens, R. Ebinghaus, and O. Vasiliev [eds.], Global and regional mercury cycles: sources, fluxes and mass balances. Kluwer Academic.

———, B. Averty, and N. Pirrone. 2009. The origin of methylmercury in open Mediterranean waters. Limnol. Oceanogr. **54:** 837–844.

Covelli, S., J. Faganeli, C. De Vittor, S. Predonzani, A. Acquavita, and M. Horvat. 2008. Benthic fluxes of mercury species in a lagoon environment (Grado Lagoon, northern Adriatic Sea, Italy). Appl. Geochem. **23:** 529–546, doi:10.1016/j.apgeochem.2007.12.011

———, ———, M. Horvat, and A. Brambati. 1999. Pore-water distribution and benthic flux measurements of mercury and methylmercury in the Gulf of Trieste (northern Adriatic Sea). Est. Coast. Shelf Sci. **48:** 415–428, doi:10.1006/ecss.1999.0466

Deonarine, A., and H. Hsu-Kim. 2009. Precipitation of mercuric sulfide nanoparticles in NOM-containing water: Implications for the natural environment. Environ. Sci. Technol. **43:** 2368–2373, doi:10.1021/es803130h

Drott, A., L. Lambertsson, E. Bjorn, and U. Skyllberg. 2007. Importance of dissolved neutral mercury sulfides for methyl mercury production in contaminated sediments. Environ. Sci. Technol. **41:** 2270–2276, doi:10.1021/es061724z

———, ———, ———, and ———. 2008*a*. Do potential methylation rates reflect accumulated methyl mercury in contaminated sediments? Environ. Sci. Technol. **42:** 153–158, doi:10.1021/es0715851

———, ———, ———, and ———. 2008*b*. Potential demethylation rate determinations in relation to concentrations of MeHg, Hg, and pore water speciation of MeHg in contaminated sediments. Mar. Chem. **112:** 93–101, doi:10.1016/j.marchem.2008.07.002

Dyrssen, D., and M. Wedborg. 1986. Titration of sulphides and thiols in natural waters. Anal. Chim. Acta **180:** 473–479, doi:10.1016/0003-2670(86)80026-5

———, and ———. 1991. The sulfur–mercury(II) system in natural waters. Water Air Soil Pollut. **56:** 507–519, doi:10.1007/BF00342295

EPA. 2001. Method 1630: Methyl mercury in water by distillation, aqueous ethylation, purge and trap, and CVAFS; EPA-821-R-01-020. Environmental Protection Agency.

———. 2002. Method 1631, Revision E: Mercury in water by oxidation, purge and trap, and cold vapor atromic fluorescence spectrometry; EPA-821-R-02-019. Environmental Protection Agency.

FAO. 2008. The State of World Fisheries and Aquaculture. Food and Agriculture Organization of the United Nations.

Gagnon, C., E. Pelletier, and A. Mucci. 1997. Behaviour of anthropogentic mercury in coastal marine sediments. Mar. Chem. **59:** 159–176, doi:10.1016/S0304-4203(97)00071-6

———, ———, ———, and W. F. Fitzgerald. 1996. Diagenetic behavior of methylmercury in organic-rich coastal sediments. Limnol. Oceanogr. **41:** 428–434, doi:10.4319/lo.1996.41.3.0428

Gill, G. A., and W. F. Fitzgerald. 1985. Mercury sampling of open ocean waters at the picomolar level. Deep-Sea Res. **32:** 287–297.

———, and ———. 1987. Picomolar mercury measurements in seawater and other materials using stannous chloride reduction and 2-stage gold amalgamation with gas-phase detection. Mar. Chem. **20:** 227–243, doi:10.1016/0304-4203(87)90074-0

———, and others. 1999. Sediment–water fluxes of mercury in Lavaca Bay, Texas. Environ. Sci. Technol. **33:** 663–669, doi:10.1021/es980380c

Gilmour, C. C., and G. S. Riedel. 1995. Measurement of Hg methylation in sediments using high specific-activity Hg-203 and ambient incubation. Water Air Soil Pollut. **80:** 747–756, doi:10.1007/BF01189726

———, ———, M. C. Ederington, J. T. Bell, J. M. Benoit, G. A. Gill, and M. C. Stordal. 1998. Methymercury concentrations and production rates across a trophic gradient in the northern Everglades. Biogeochemistry **40:** 327–345, doi:10.1023/A:1005972708616

Gobeil, C., and D. Cossa. 1993. Mercury in sediments and sediment pore-water in the Laurentian Trough. Can. J. Fish. Aquat. Sci. **50:** 1794–1800, doi:10.1139/f93-201

Goulet, R. R., and others. 2007. Mercury transformations and fluxes in sediments of a riverine wetland. Geochim. Cosmochim. Acta **71:** 3393–3406, doi:10.1016/j.gca.2007.04.032

Hammerschmidt, C. R., and W. F. Fitzgerald. 2004. Geochemical controls on the production and distribution of methylmercury in near-shore marine sediments. Environ. Sci. Technol. **38:** 1487–1495, doi:10.1021/es034528q

———, and ———. 2006. Methylmercury cycling in sediments on the continental shelf of southern New England. Geochim. Cosmochim. Acta **70:** 918–930, doi:10.1016/j.gca.2005.10.020

———, and ———. 2008. Sediment–water exchange of methylmercury determined from shipboard benthic flux chambers. Mar. Chem. **109:** 86–97, doi:10.1016/j.marchem.2007.12.006

———, ———, P. H. Balcom, and P. T. Visscher. 2008. Organic matter and sulfide inhibit methylmercury production in sediments of New York/New Jersey Harbor. Mar. Chem. **109:** 165–182, doi:10.1016/j.marchem.2008.01.007

———, ———, C. H. Lamborg, P. H. Balcom, and P. T. Visscher. 2004. Biogeochemistry of methylmercury in sediments of Long Island Sound. Mar. Chem. **90:** 31–52, doi:10.1016/j.marchem.2004.02.024

Han, S., A. Obraztsova, P. Pretto, D. D. Deheyn, J. Gieskes, and B. M. Tebo. 2008. Sulfide and iron control on mercury speciation in anoxic estuarine sediment slurries. Mar. Chem. **111:** 214–220, doi:10.1016/j.marchem.2008.05.002

Hayduk, W., and H. Laudie. 1974. Prediction of diffusion coefficients for nonelectrolytes in dilute aqueous solutions. Am. Inst. Chem. Eng. **20:** 611–615.

Heyes, A., R. P. Mason, E.-H. Kim, and E. Sunderland. 2006. Mercury methylation in estuaries: Insights from using measuring rates using stable mercury isotopes. Mar. Chem. **102:** 134–147, doi:10.1016/j.marchem.2005.09.018

Hintelmann, H., and R. D. Evans. 1997. Application of stable isotopes in environmental tracer studies—measurement of monomethylmercury (CH3Hg+) by isotope dilution ICP-MS and detection of species transformation. Fres. J. Anal. Chem. **358:** 378–385, doi:10.1007/s002160050433

———, K. Keppel-Jones, and R. D. Evans. 2000. Constants of mercury methylation and demethylation rates in sediments and comparison of tracer and ambient mercury availability. Environ. Toxicol. Chem. **19:** 2204–2211, doi:10.1002/etc.5620190909

———, AND N. OGRINC. 2003. Determination of stable mercury isotopes by ICP/MS and their application in environmental studies, p. 321–338, Biogeochemistry of Environmentally Important Trace Elements. ACS Symposium Series.

HOLLWEG, T. A. 2010. Mercury cycling in sediments of Chesapeake Bay and the Mid-Atlantic continental shelf and slope. Ph.D. thesis. University of Connecticut.

———, C. C. GILMOUR, AND R. P. MASON. 2009. Methylmercury production in sediments of Chesapeake Bay and the mid-Atlantic continental margin. Mar. Chem. **114:** 86–101, doi:10.1016/j.marchem.2009.04.004

HSU-KIM, H., AND D. L. SEDLAK. 2005. Similarities between inorganic sulfide and the strong Hg(II)—complexing ligands in municipal wastewater effluent. Environ. Sci. Technol. **39:** 4035–4041, doi:10.1021/es050013i

JAHNKE, R., M. RICHARDS, J. NELSON, C. ROBERTSON, A. RAO, AND D. JAHNKE. 2005. Organic matter remineralization and porewater exchange rates in permeable South Atlantic Bight continental shelf sediments. Cont. Shelf Res. **25:** 1433–1452, doi:10.1016/j.csr.2005.04.002

KARLSSON, T., AND U. SKYLLBERG. 2003. Bonding of ppb levels of methyl mercury to reduced sulfur groups in soil organic matter. Environ. Sci. Technol. **37:** 4912–4918, doi:10.1021/es034302n

KIM, E. H., R. P. MASON, E. T. PORTER, AND H. L. SOULEN. 2006. The impact of resuspension on sediment mercury dynamics, and methylmercury production and fate: A mesocosm study. Mar. Chem. **102:** 300–315, doi:10.1016/j.marchem.2006.05.006

KIRK, J. L., V. L. S. LOUIS, H. HINTELMANN, I. LEHNHERR, B. ELSE, AND L. POISSANT. 2008. Methylated mercury species in marine waters of the Canadian high and sub-Arctic. Environ. Sci. Technol. **42:** 8367–8373, doi:10.1021/es801635m

LAURIER, F. J. G., D. COSSA, J. L. GONZALEZ, E. BREVIERE, AND G. SARAZIN. 2003. Mercury transformations and exchanges in a high turbidity estuary: The role of organic matter and amorphous oxyhydroxides. Geochim. Cosmochim. Acta **67:** 3329–3345, doi:10.1016/S0016-7037(03)00081-4

LI, Y.-H., AND S. GREGORY. 1974. Diffusion of ions in sea water and in deep-sea sediments. Geochim. Cosmochim. Acta **38:** 703–714, doi:10.1016/0016-7037(74)90145-8

LIU, B., AND OTHERS. 2009. Disturbance impacts on mercury dynamics in northern Gulf of Mexico sediments. J. Geophys. Res. Biogeosci. **114:** G00C07, doi:10.1029/2008JG000752

MARTIN-DOIMEADIOS, R. C., E. TESSIER, D. AMOUROUX, R. GUYONEAUD, R. DURAN, P. CAUMETTE, AND O. F. X. DONARD. 2004. Mercury methylation/demethylation and volatilization pathways in estuarine sediment slurries using species-specific enriched stable isotopes. Mar. Chem. **90:** 107–123, doi:10.1016/j.marchem.2004.02.022

MARVIN-DIPASQUALE, M., J. AGEE, C. MCGOWAN, R. S. OREMLAND, M. THOMAS, D. KRABBENHOFT, AND C. C. GILMOUR. 2000. Methyl-mercury degradation pathways: A comparison among three mercury-impacted ecosystems. Environ. Sci. Technol. **34:** 4908–4916, doi:10.1021/es0013125

MASON, R. P., AND J. M. BENOIT. 2003. Organomercury compounds in the environment, p. 57–99. *In* P. Craig [ed.], Organometallic compounds in the environment. Wiley.

———, AND W. F. FITZGERALD. 1993. The distribution and biogeochemical cycling of mercury in the equatorial Pacific Ocean. Deep-Sea Res. I **40:** 1897–1924, doi:10.1016/0967-0637(93)90037-4

———, N. M. LAWSON, A. L. LAWRENCE, J. J. LEANER, J. G. LEE, AND G.-R. SHEU. 1999. Mercury in Chesapeake Bay. Mar. Chem. **65:** 77–96, doi:10.1016/S0304-4203(99)00012-2

———, AND G. R. SHEU. 2002. Role of the ocean in the global mercury cycle. Glob. Biogeochem. Cycles **16:** 1093, doi:10.1029/2001GB001440

MERGLER, D., H. A. ANDERSON, L. H. M. CHAN, K. R. MAHAFFEY, M. MURRAY, M. SAKAMOTO, AND A. H. STERN. 2007. Methylmercury exposure and health effects in humans: A worldwide concern. Ambio **36:** 3–11, doi:10.1579/0044-7447(2007)36[3:MEAHEI]2.0.CO;2

MIKAC, N., S. NIESSEN, B. OUDDANE, AND M. WARTEL. 1999. Speciation of mercury in sediments of the Seine estuary (France). Appl. Organomet. Chem. **13:** 715–725, doi:10.1002/(SICI)1099-0739(199910)13:10<715::AID-AOC918>3.0.CO;2-4

MILLER, C. L., R. P. MASON, C. C. GILMOUR, AND A. HEYES. 2007. Influence of dissolved organic matter on the complexation of mercury under sulfidic conditions. Environ. Toxicol. Chem. **26:** 624–633, doi:10.1897/06-375R.1

MITCHELL, C. P. J., AND C. C. GILMOUR. 2008. Methylmercury production in a Chesapeake Bay salt marsh. J. Geophys. Res. Biogeosci. **113:** G00C04, doi:10.1029/2008JG000765

MONPERRUS, M., E. TESSIER, D. AMOUROUX, A. LEYNAERT, P. HUONNIC, AND O. F. X. DONARD. 2007*a*. Mercury methylation, demethylation and reduction rates in coastal and marine surface waters of the Mediterranean Sea. Mar. Chem. **107:** 49–63, doi:10.1016/j.marchem.2007.01.018

———, AND OTHERS. 2007*b*. The biogeochemistry of mercury at the sediment–water interface in the Thau Lagoon. 2. Evaluation of mercury methylation potential in both surface sediment and the water column. Est. Coast. Shelf Sci. **72:** 485–496, doi:10.1016/j.ecss.2006.11.014

MOREL, F. M. M., AND J. G. HERING. 1993. Principles and applications of aquatic chemistry. Wiley.

MUNTHE, J., AND OTHERS. 2007. Recovery of mercury-contaminated fisheries. Ambio **36:** 33–44, doi:10.1579/0044-7447(2007)36[33:ROMF]2.0.CO;2

MURESAN, B., D. COSSA, D. JEZEQUEL, F. PREVOT, AND S. KERBELLEC. 2007. The biogeochemistry of mercury at the sediment–water interface in the Thau lagoon. 1. Partition and speciation. Est. Coast. Shelf Sci. **72:** 472–484, doi:10.1016/j.ecss.2006.11.015

OGRINC, N., AND OTHERS. 2007. Distribution of mercury and methylmercury in deep-sea surficial sediments of the Mediterranean Sea. Mar. Chem. **107:** 31–48, doi:10.1016/j.marchem.2007.01.019

OREMLAND, R. S., C. W. CULBERTSON, AND M. R. WINFREY. 1991. Methylmercury decomposition in sediments and bacterial cultures—involvement of methanogens and sulfate reducers in oxidative demethylation. Appl. Environ. Microbiol. **57:** 130–137.

POINT, D., AND OTHERS. 2007. Biological control of trace metal and organometal benthic fluxes in a eutrophic lagoon (Thau Lagoon, Mediterranean Sea, France). Est. Coast. Shelf Sci. **72:** 457–471, doi:10.1016/j.ecss.2006.11.013

QIAN, J., U. SKYLLBERG, W. FRECH, W. F. BLEAM, P. R. BLOOM, AND P. E. PETIT. 2002. Bonding of methyl mercury to reduced sulfur groups in soil and stream organic matter as determined by X-ray absorption spectroscopy and binding affinity studies. Geochim. Cosmochim. Acta **66:** 3873–3885, doi:10.1016/S0016-7037(02)00974-2

RAVICHANDRAN, M. 2004. Interactions between mercury and dissolved organic matter—a review. Chemosphere **55:** 319–331, doi:10.1016/j.chemosphere.2003.11.011

ROTHENBERG, S. E., R. F. AMBROSE, AND J. A. JAY. 2008. Mercury cycling in surface water, pore water and sediments of Mugu Lagoon, CA, USA. Environ. Pollut. **154:** 32–45, doi:10.1016/j.envpol.2007.12.013

SCHECHER, W., AND D. MCAVOY. 2001. MINEQL+, user's manual. http://www.mineql.com/

Schnoor, J. L. 1996. Environmental modeling: Fate of chemicals in water, air and soil. Wiley.

Schwarzenbach, G., and S. M. Schellenberg. 1965. Die komplexchemie des methylquecksilber-kations. Helv. Chim. Acta **48:** 28. [The complexes of methylmercury cations.], doi:10.1002/hlca.19650480104

———, and M. Widmer. 1963. Die loslichkeit von metallsulfiden 1. Schwarzes quecksilbersulfid. Helv. Chim. Acta **46:** 2613–2628[The solubility of metal sulfides I. Black mercury sulfide.], doi:10.1002/hlca.19630460719

Schwarzenbach, R. P., P. M. Gschwend, and D. M. Imboden. 1993. Environmental organic chemistry. Wiley.

Skyllberg, U. 2008. Competition among thiols and inorganic sulfides and polysulfides for Hg and MeHg in wetland soils and sediments under suboxic conditions: Illumination of controversies and implications for MeHg net production. J. Geophys. Res. Biogeosci. **113:** G00C03, doi:10.1029/2008JG000745

Stumm, W., and J. J. Morgan. 1996. Aquatic chemistry, 3rd ed. Wiley.

Sunderland, E. M. 2007. Mercury exposure from domestic and imported estuarine and marine fish in the US seafood market. Environ. Health Perspect. **115:** 235–242, doi:10.1289/ehp.9377

———, J. Dalziel, A. Heyes, B. A. Branfireun, D. P. Krabbenhoft, and F. Gobas. 2010. Response of a macrotidal estuary to changes in anthropogenic mercury loading between 1850 and 2000. Environmental Science & Technology **44:** 1698–1704, doi:10.1021/es9032524

———, F. Gobas, B. A. Branfireun, and A. Heyes. 2006. Environmental controls on the speciation and distribution of mercury in coastal sediments. Mar. Chem. **102:** 111–123, doi:10.1016/j.marchem.2005.09.019

———, F.A.P.C. Gobas, A. Heyes, B. A. Branfireun, A. K. Bayer, R. E. Cranston, and M. B. Parsons. 2004. Speciation and bioavailability of mercury in well-mixed estuarine sediments. Mar. Chem. **90:** 91–105, doi:10.1016/j.marchem.2004.02.021

———, D. P. Krabbenhoft, J. W. Moreau, S. A. Strode, and W. M. Landing. 2009. Mercury sources, distribution, and bioavailability in the North Pacific Ocean: Insights from data and models. Glob. Biogeochem. Cycles **23:** GB2010, doi:10.1029/2008GB003425

———, and R. P. Mason. 2007. Human impacts on open ocean mercury concentrations. Glob. Biogeochem. Cycles **21:** GB4022, doi:10.1029/2006GB002876

Thomas, C. J., N. E. Blair, M. J. Alperin, D. J.DeMaster, R. A. Jahnke, C. S. Martens, and L. Mayer. 2002. Organic carbon deposition on the North Carolina continental slope off Cape Hatteras (USA). Deep-Sea Res. II **49:** 4687–4709, doi:10.1016/S0967-0645(02)00135-2

Warnken, K. W., G. A. Gill, P. H. Santschi, and L. L. Griffin. 2000. Benthic exchange of nutrients in Galveston Bay, Texas. Estuaries **23:** 647–661, doi:10.2307/1352891

Whalin, L., E. H. Kim, and R. Mason. 2007. Factors influencing the oxidation, reduction, methylation and demethylation of mercury species in coastal waters. Mar. Chem. **107:** 278–294, doi:10.1016/j.marchem.2007.04.002

Associate editor: Robert E. Hecky

Received: 22 February 2010
Accepted: 31 August 2010
Amended: 14 September 2010